

Vast Volatility Matrix Estimation using High Frequency Data for Portfolio Selection *

Jianqing Fan, Yingying Li, Ke Yu
Princeton University, HKUST, Princeton University

April 29, 2010

Abstract

Portfolio allocation with gross-exposure constraint is an effective method to increase the efficiency and stability of selected portfolios among a vast pool of assets, as demonstrated in Fan *et al.* (2008b). The required high-dimensional volatility matrix can be estimated by using high frequency financial data. This enables us to better adapt to the local volatilities and local correlations among vast number of assets and to increase significantly the sample size for estimating the volatility matrix. This paper studies the volatility matrix estimation using high-dimensional high-frequency data from the perspective of portfolio selection. Specifically, we propose the use of “pairwise-refresh time” and “all-refresh time” methods proposed by Barndorff-Nielsen *et al.* (2008) for estimation of vast covariance matrix and compare their merits in the portfolio selection. We also establish the concentration inequalities of the estimates, which guarantee desirable properties of the estimated volatility matrix in vast asset allocation with gross exposure constraints. Extensive numerical studies are made via carefully designed simulations. Comparing with the methods based on low frequency daily data, our methods can capture the most recent trend of the time varying volatility and correlation, hence provide more accurate guidance for the portfolio allocation in the next time period. The advantage of using high-frequency data is significant in our simulation and empirical studies, which consist of 50 simulated assets and 30 constituent stocks of Dow Jones Industrial Average index.

KEY WORDS: Minimum variance portfolio, portfolio allocation, risk assessment, refresh time, volatility matrix estimation, high frequency data.

*The paper was supported by the NSF Grants DMS-0704337 and DMS-0714554. The main part of the work was carried while Yingying Li was a postdoctoral fellow at Department of Operations Research and Financial Engineering, Princeton University. Yingying Li was further supported by the Research Support Fund from the ISOM Department at Hong Kong University of Science and Technology. **Address Information:** Jianqing Fan, Bendheim Center for Finance, Princeton University, 26 Prospect Avenue, Princeton, NJ 08540, USA. E-mail: jqfan@princeton.edu. Yingying Li, Department of Information Systems, Business Statistics and Operations Management, Hong Kong University of Science and Technology, Hong Kong. E-mail: yyli@ust.hk. Ke Yu, Department of Operations Research and Financial Engineering, Princeton University, Princeton, NJ 08540. E-mail: kyu@Princeton.edu.

1 Introduction

The mean-variance efficient portfolio theory by Markowitz (1952, 1959) has profound impact on modern finance. Yet, its applications to practical portfolio selection face a number of challenges. It is well known that the selected portfolios depend too sensitively on the expected future returns and volatility matrix (Klein and Bawa, 1976; Best and Grauer, 1991; Chopra and Ziemba, 1993). This leads to the puzzle postulated by Jagannathan and Ma (2003) why no short-sale portfolio outperforms the efficient Markowitz portfolio. See also De Roon, *et al.* (2001) on the study of optimal no-short sale portfolio on emerging market. The sensitivity on the dependence can be effectively addressed by the introduction of the constraint on the gross exposure of portfolios (Fan *et al.*, 2008b). In particular, Fan *et al.* (2008b) shows, with non-asymptotic inequalities, that for a range of gross exposure constraint parameters, the actual risk of an empirically selected optimal portfolio, the actual risk of the theoretically optimal portfolio, and the estimated risk of an empirically selected optimal portfolio are in fact close. The accuracy depends only on the gross exposure parameter and the maximum componentwise estimation error of expected returns and covariance matrix — there is little error accumulation effect. The results are demonstrated also by both simulation and empirical studies. This gives not only a theoretical answer to the puzzle postulated by Jagannathan and Ma (2003) but also paves a way for optimal portfolio selection in practice.

The second challenge of the implementation of Markowitz's portfolio selection theory is the intrinsic difficulty of the estimation of the large volatility matrix. This is well documented in the statistics and econometrics literature even for the static large covariance matrix (Johnstone, 2001; Bickel and Levina, 2008; Fan, *et al.*, 2008a; Lam and Fan, 2009; Rothman *et al.*, 2009). The additional challenge comes from the time-varying nature of a large volatility matrix. For a short and medium holding period (one day or one week, say), the expected volatility matrix in the near future can be very different from the average of the expected volatility matrix over a long time horizon (the past one year, say). As a result, even if we know exactly the realized volatility matrix in the past, the bias can still be large. This calls for a stable and robust portfolio selection. The portfolio allocation under the gross exposure constraint provides a needed solution. To reduce the bias of the forecasted expected volatility matrix, we need to shorten the learning period to better capture the dynamics of the time-varying volatility matrix, adapting better to the local volatility and correlation. But this is at the expense of a reduced sample size. The wide availability of high-frequency data provides sufficient amount of data for reliable estimation of the volatility matrix.

Recent years have seen dramatic developments in the study of high frequency data in integrated volatility. Statisticians and econometricians have been focusing on the interesting and challenging problem of volatility estimation in the presence of market microstructure noise and asynchronous tradings, which are the style features of high-frequency financial data. The progresses are very

impressive with a large literature. Assuming the price processes follow Brownian semimartingales to satisfy the no-arbitrage based characterizations (Delbaen and Schachermayer, 1994), if there were no market microstructure noise, and if the processes are observed synchronously on grids that become denser, classical results in stochastic calculus show that the realized variance and realized covariance are consistent estimators of the quadratic variation and quadratic co-variation of two price processes; see for example Karatzas and Shreve (2000) and Jacod and Shiryaev (2003). When directly applied to high-frequency financial data, however, Andersen *et al.* (2000) show that the realized variance exhibits a large positive bias when the sampling frequency gets higher, through their famous signature plots; Epps (1979) documented that the correlation estimates based on the realized covariances tend to be biased toward zero when sampled at high frequencies. The recent developments have enabled us to understand much better the signature plots and Epps effect. Analytical explanations of how the market microstructure noise and asynchronization may affect the estimates and ways to correct for the biases have been given. In particular, in the one dimensional case when the focus is on estimation of integrated volatility, Aït-Sahalia, *et al.* (2005) discussed a subsampling scheme; Zhang, *et al.* (2005) proposed a two-scale estimate which was extended and improved by Zhang (2006) to multiple scales; Fan and Wang (2007) separated jumps from diffusions in presence of market microstructural noise using a wavelet method; the robustness issues are addressed by Li and Mykland (2007); the realized kernel methods are proposed and thoroughly studied in Barndorff-Nielsen *et al.* (2009a,b); Jacod, *et al.* (2009) proposed a pre-averaging approach to reduce the market microstructural noise; Xiu (2008) demonstrated that a simple quasi-likelihood method achieves the optimal rate of convergence for estimating integrated volatility. For estimation of integrated covariation, the non-synchronized trading issue was first addressed by Hayashi and Yoshida (2005) in absence of the microstructural noise; the kernel method with refresh time idea was first proposed by Barndorff-Nielsen *et al.* (2008); Zhang (2009) extend the two-scale method to study the integrated covariation using a previous tick method; Wang, *et al.* (2009) aggregate daily integrated volatility matrix via a factor model; Aït-Sahalia, *et al.* (2010) extend the quasi-maximum likelihood method; Kinnebrock *et al.* (2009) extend the pre-averaging technique.

The aim of this paper is to study the volatility matrix estimation using high-dimensional high-frequency data from the perspective of financial engineering. Specifically, our main topic is how to extract the covariation information from high-frequency data for asset allocation and how effective they are. Two particular strategies are proposed for handling the non-synchronized trading: “pairwise-refresh” and “all-refresh” schemes. The former retains much more data points and estimates covariance matrix componentwise, which is usually not semi-positive definite, whereas the latter retains far less data points and the resulting covariance matrix is usually semi-positive definite. As a result, the former has a better componentwise estimation error and is better in controlling risk approximation mentioned in the first paragraph of the introduction. However, the merits between the two methods are not that simple. In implementation, quadratic programming algorithms require the estimated covariance matrix to be semi-positive definite. Therefore, we need to project

the estimate of covariance matrix based on the “pairwise-refresh” scheme onto the space of the semi-positive definite matrices. However, the projections distort the accuracy of the elementwise estimation. As a result, the pairwise-refresh scheme does not have much more advantage than the all-refresh method, though the former is very easy to implement. However, both methods significantly outperform the methods based on low frequency data, since they adapt better to the time-varying volatilities and correlations. The comparative advantage is more dramatic when there are rapid changes of the volatility matrix over time. This will be demonstrated in both simulation and empirical studies.

As mentioned in the introduction and demonstrated in Section 2, the accuracy of portfolio risk relative to the theoretically optimal portfolio is governed by the maximum elementwise estimation error. How does this error grow with the number of assets? Thanks to the concentration inequalities derived in this paper, it grows only at the logarithmic order of the number of assets. This gives a theoretical endorsement why the portfolio selection problem is feasible for vast portfolios.

The paper is organized as follows. Section 2 gives an overview of portfolio allocation using high-frequency data. Section 3 studies the volatility matrix estimation using high-frequency data from the perspective of asset allocation, where the analytical results are also presented. How well our idea works in simulation and empirical studies can be found in Sections 3 and 4, respectively. Conclusions are given in Section 5. Technical conditions and proofs are relegated to the appendix.

2 Constrained Portfolio Optimization with High Frequency Data

2.1 Problem Setup

Consider a pool of p assets, with log-price processes $X_t^{(1)}, X_t^{(2)}, \dots, X_t^{(p)}$. Denote by $\mathbf{X}_s = (X_s^{(1)}, \dots, X_s^{(p)})^T$ the vector of the log-price processes at time s . Suppose they follow an Itô process, namely,

$$d\mathbf{X}_t = \boldsymbol{\mu}_t dt + \mathbf{S}_t^{1/2} d\mathbf{W}_t \quad (1)$$

where \mathbf{W}_t is the vector of p -dimensional standard Brownian motions. The drift vector $\boldsymbol{\mu}_t$ and the instantaneous variance \mathbf{S}_t can be stochastic processes and are assumed to be bounded and independent of \mathbf{W}_t .

A given portfolio with the allocation vector \mathbf{w} at time t and a holding period τ has the log-return $\mathbf{w}^T \int_t^{t+\tau} dX_s$ with variance (risk)

$$R_{t,\tau}(\mathbf{w}) = \mathbf{w}^T \boldsymbol{\Sigma}_{t,\tau} \mathbf{w}, \quad (2)$$

where $\mathbf{w}^T \mathbf{1} = 1$ and

$$\boldsymbol{\Sigma}_{t,\tau} = \int_t^{t+\tau} E_t \mathbf{S}_u du \quad (3)$$

with E_t denoting the conditional expectation given the history up to time t . Let w^+ be the proportion of long positions and w^- be the proportion of the short positions. Then, $\|\mathbf{w}\|_1 = w_+ + w_-$ is the gross exposure of the portfolio. To simplify the problem, following Jagannathan and Ma (2003) and Fan *et al.* (2008b) and other papers in the literature, we consider only the risk optimization problem. In practice, the expected return constraint can be replaced by the constraints of sectors or industries, to avoid unreliable estimates of the expected return vector. For a short-time horizon, the expected return is usually negligible. Following Fan *et al.* (2008b), we consider the following risk optimization under gross exposure constraints:

$$\min \mathbf{w}^T \boldsymbol{\Sigma}_{t,\tau} \mathbf{w}, \quad s.t. \|\mathbf{w}\|_1 \leq c \text{ and } \mathbf{w}^T \mathbf{1} = 1, \quad (4)$$

where c is the total exposure allowed. Note that using $w^+ - w^- = 1$, the problem (4) puts equivalently the constraint on the proportion of the short positions: $w^- \leq (c - 1)/2$.

Problem (4) involves the conditional expected volatility matrix (3) in the future. Unless we know exactly the dynamic of the volatility process, this is usually unknown, even if we observed the entire continuous paths up to the current time t . As a result, we rely on the approximation even with ideal data that we were able to observe the processes continuously without error. The typical approximation is

$$\tau^{-1} \boldsymbol{\Sigma}_{t,\tau} \approx h^{-1} \int_{t-h}^t \mathbf{S}_u du, \quad (5)$$

for an appropriate window width h and we estimate $\int_{t-h}^t \mathbf{S}_u du$ based on the historical data at the time interval $[t - h, t]$.

The approximation (5) holds reasonably well when τ and h are both small. This relies on the continuity assumptions: local time-varying volatility matrices are continuous in τ . The approximation is also reasonable when both τ and h are large. This relies on the stationarity assumption so that both quantity will be approximately $E\mathbf{S}_u$, when the stochastic volatility matrix \mathbf{S}_u is stationary. The approximation is not good when τ is small whereas h is large as long as \mathbf{S}_u is time varying, whether or not the stochastic volatility \mathbf{S}_u is stationary or not. In other words, when the holding time horizon τ is short, as long as \mathbf{S}_u is time varying, we can only use a short time window $[t - h, t]$ to estimate $\boldsymbol{\Sigma}_{t,\tau}$. The recent arrivals of high-frequency data make this problem feasible.

The approximation error in (5) can not usually be evaluated unless we have a specific parametric model on the stochastic volatility matrix \mathbf{S}_u . However, this is at the risk of model misspecifications and nonparametric approach is usually preferred for high-frequency data. With p^2 elements are approximated, which can be in the order of hundred of thousands or millions, a natural question to ask is whether these errors accumulate and whether the result (risk) is stable. The gross-exposure constraint gives a stable solution to the problem as shown in Fan *et al.* (2008b).

2.2 Risk approximations with gross exposure constraints

The utility of gross-exposure constraint can easily be seen through the following inequality. Let $\hat{\Sigma}_{t,\tau}$ be an estimated covariance matrix and

$$\hat{R}_{t,\tau}(\mathbf{w}) = \mathbf{w}^T \hat{\Sigma}_{t,\tau} \mathbf{w} \quad (6)$$

be estimated risk of the portfolio. Then, for any portfolio with gross-exposure $\|\mathbf{w}\|_1 \leq c$, we have

$$\begin{aligned} |\hat{R}_{t,\tau}(\mathbf{w}) - R_{t,\tau}(\mathbf{w})| &\leq \sum_{i=1}^p \sum_{j=1}^p |\hat{\sigma}_{i,j} - \sigma_{i,j}| |w_i| |w_j| \\ &\leq \|\Sigma_{t,\tau} - \hat{\Sigma}_{t,\tau}\|_\infty \|\mathbf{w}\|_1^2 \\ &\leq \|\Sigma_{t,\tau} - \hat{\Sigma}_{t,\tau}\|_\infty c^2, \end{aligned} \quad (7)$$

where $\hat{\sigma}_{i,j}$ and $\sigma_{i,j}$ are respectively the (i,j) elements of $\hat{\Sigma}_{t,\tau}$ and $\Sigma_{t,\tau}$, and

$$\|\Sigma_{t,\tau} - \hat{\Sigma}_{t,\tau}\|_\infty = \max_{i,j} |\hat{\sigma}_{i,j} - \sigma_{i,j}|$$

is the maximum componentwise estimation error. The risk approximation (7) reveals that there is no error accumulation effect when gross exposure c is moderate.

From now on, we drop the dependence of t and τ whenever there is no confusion. This facilitates the notation.

Fan *et al.* (2008b) showed further that the risks of optimal portfolios are indeed close. Let

$$\mathbf{w}_{opt} = \operatorname{argmin}_{\mathbf{w}^T \mathbf{1}=1, \|\mathbf{w}\|_1 \leq c} R(\mathbf{w}), \quad \hat{\mathbf{w}}_{opt} = \operatorname{argmin}_{\mathbf{w}^T \mathbf{1}=1, \|\mathbf{w}\|_1 \leq c} \hat{R}(\mathbf{w}) \quad (8)$$

be respectively the theoretical (oracle) optimal allocation vector we want and the estimated optimal allocation vector we get. Then, $R(\mathbf{w}_{opt})$ is the theoretical minimum risk and $R(\hat{\mathbf{w}}_{opt})$ is the actual risk of our selected portfolio, whereas $\hat{R}(\hat{\mathbf{w}}_{opt})$ is our perceived risk, which is the quantity known to financial econometricians. They showed that

$$|R(\hat{\mathbf{w}}_{opt}) - R(\mathbf{w}_{opt})| \leq 2a_p c^2, \quad (9)$$

$$|R(\hat{\mathbf{w}}_{opt}) - \hat{R}(\hat{\mathbf{w}}_{opt})| \leq a_p c^2, \quad (10)$$

$$|R(\mathbf{w}_{opt}) - \hat{R}(\hat{\mathbf{w}}_{opt})| \leq a_p c^2. \quad (11)$$

with $a_p = \|\hat{\Sigma} - \Sigma\|_\infty$, which usually grows slowly with the number of assets p . These reveal that the three relevant risks are in fact close as long as the gross-exposure parameter c is moderate and the maximum componentwise estimation error a_p is small.

The above risk approximations hold for any estimate of covariance matrix. It does not even

require $\hat{\Sigma}$ a semi-positive definite matrix. This facilitates significantly the method of covariance matrix estimation. In particular, the elementwise estimation methods are allowed. In fact, since the approximation errors in (9), (10) and (11) are all controlled by the maximum elementwise estimation error, it can be advantageous to use elementwise estimation methods. This is particularly the case for the high-frequency data where trading are non-synchronized. The synchronization can be done pairwise or for all assets. The former retains much more data than the latter, as shown in the next section.

3 Estimation of Covariance Matrix Using High Frequency Data

3.1 All-refresh method and pairwise-refresh method

Estimating high-dimensional volatility matrix using high-frequency data is a challenging task. One of the challenges is the non-synchronicity of trading. Several synchronization schemes have been proposed. The refresh time method is proposed in Barndorff-Nielsen *et al.* (2008) and the previous tick method is proposed in Zhang (2009). The former uses more efficiently the available data and will be used in this paper.

The idea of refresh time is to wait until all assets are traded at least once at time v_1 (say) and then use the last price traded before or at v_1 of each asset as its price at time v_1 . This obtains one synchronized price vector at time v_1 . The clock now starts again. Wait until all assets are traded at least once at time v_2 (say) and again use the previous tick price of each asset as its price at time v_2 . This yields the second synchronized price vector at time v_2 . Repeat the process until all available trading data are synchronized. Clearly, the process discards a large portion of the available trades: After each synchronization, we always wait until the slowest stock to trade once. But this is the most efficient synchronization scheme. We will refer this synchronorization scheme as the “all-refresh time” (The method is called all-refresh method for short). Barndorff-Nielsen *et al.* (2008) advocate the kernel method to estimate integrated volatility matrix after synchronization, but this can also be done by using other methods. The advantage of the all-refresh method is that the estimated covariance matrix can be made semi-positive definite.

A more efficient method to use the available sample is the pairwise refresh time scheme, which synchronizes the trading for each pair of assets separately (The method is called pairwise-refresh method for short). This retains far more data points, but we have to estimate the covariance matrix elementwise. The resulting covariance matrix is not necessarily semi-positive definite. Thanks to the gross exposure constraint, this is still applicable to the portfolio selection problems, as long as the elementwise estimation error is small. See (7) – (11). The pairwise-refresh scheme makes far more efficient use of the rich information in high-frequency data, and enables us to estimate each element in the volatility matrix more precisely, which helps improve the efficiency of the selected

portfolio. We will study the merits of these two methods.

The pairwise estimation method allows us to use a wealth of univariate integrated volatility estimators, such as the two-scale realized volatility (TSRV) (Zhang, *et al.*, 2005), the multi-scale realized volatility (MSRV) (Zhang, 2006), the wavelet method (Fan and Wang, 2007), the realized kernel method (Barndorff-Nielsen *et al.*, 2009a,b), the pre-averaging approach (Jacod, *et al.*, 2009) and the QMLE method (Xiu, 2008). For any given two assets with log-price processes $X_t^{(i)}$ and $X_t^{(j)}$, with pairwise-refresh times, the synchronized prices of $X_t^{(i)} + X_t^{(j)}$ and $X_t^{(i)} - X_t^{(j)}$ can be computed. With the univariate estimate of the integrated volatilities $\langle X^{(i)} + X^{(j)} \rangle$ and $\langle X^{(i)} - X^{(j)} \rangle$, the integrated covariation can be estimated as

$$\hat{\sigma}_{i,j} = \langle X^{(i)}, Y^{(j)} \rangle = (\langle X^{(i)} + X^{(j)} \rangle - \langle X^{(i)} - X^{(j)} \rangle)/4. \quad (12)$$

In particular, the diagonal elements are estimated by the method itself. When the TSRV is used, this results in the two-scale realized covariance (TSCV) estimate (Zhang, 2009).

3.2 Pairwise refresh method and TSCV

We now focus on the pairwise estimation method. To facilitate the notation, we reintroduce it.

We consider two log price processes X and Y that satisfy

$$dX_t = \mu_t^{(X)} dt + \sigma_t^{(X)} dB^{(X)} \quad \text{and} \quad dY_t = \mu_t^{(Y)} dt + \sigma_t^{(Y)} dB^{(Y)}, \quad (13)$$

where $\text{cor}(B_t^{(X)}, B_t^{(Y)}) = \rho_t^{(X,Y)}$. For the two processes X and Y , consider the problem of estimating $\langle X, Y \rangle_T$ with $T = 1$. Denote by \mathcal{T}_n the observation times of X and \mathcal{S}_m the observation times of Y . Denote the elements in \mathcal{T}_n and \mathcal{S}_m by $\{\tau_{n,i}\}_{i=0}^n$ and $\{\theta_{m,i}\}_{i=0}^m$ respectively, in an ascending order ($\tau_{n,0}$ and $\theta_{m,0}$ are set to be 0). We assume that the actual log-prices are not observable, but are observed with microstructure noises:

$$X_{\tau_{n,i}}^o = X_{\tau_{n,i}} + \epsilon_i^X, \quad \text{and} \quad Y_{\theta_{m,i}}^o = Y_{\theta_{m,i}} + \epsilon_i^Y \quad (14)$$

where X^o and Y^o are the observed transaction prices in the logarithmic scale, and X and Y are the latent log prices govern by the stochastic dynamics (13). We assume that the microstructure noise ϵ_i^X and ϵ_i^Y processes are independent of the X and Y processes and that

$$\epsilon_i^X \sim_{i.i.d.} N(0, \eta_X^2) \quad \text{and} \quad \epsilon_i^Y \sim_{i.i.d.} N(0, \eta_Y^2). \quad (15)$$

Note that this assumption is mainly for the simplicity of presentation; as we can see from the proof, one can for example easily replace the Gaussian assumption with the sub-Gaussian assumption without affecting our results.

The pairwise refresh time $\mathcal{V} = \{v_0, v_1, \dots, v_{\tilde{n}}\}$ can be obtained by setting $v_0 = 0$, and

$$v_i = \max \left\{ \min\{\tau \in \mathcal{T}_n : \tau > v_{i-1}\}, \min\{\theta \in \mathcal{S}_m : \theta > v_{i-1}\} \right\},$$

where \tilde{n} is the total number of refresh times in the interval $(0, 1]$. The actual sample times for the two individual processes X and Y that correspond to the refresh times are

$$t_i = \max\{\tau \in \mathcal{T}_n : \tau \leq v_i\} \text{ and } s_i = \max\{\theta \in \mathcal{S}_m : \theta \leq v_i\},$$

which is really the previous-tick measurement.

We study the property of the TSCV based on the *asynchronous* data:

$$\widehat{\langle X, Y \rangle}_1 = [X^o, Y^o]_1^{(K)} - \frac{\bar{n}_K}{\bar{n}_J} [X^o, Y^o]_1^{(J)}, \quad (16)$$

where

$$[X^o, Y^o]_1^{(K)} = \frac{1}{K} \sum_{i=K}^{\tilde{n}} (X_{t_i}^o - X_{t_{i-K}}^o)(Y_{s_i}^o - Y_{s_{i-K}}^o)$$

and $\bar{n}_K = (\tilde{n} - K + 1)/K$. As discussed in Zhang (2009), the optimal choice of K has order $K = O(\tilde{n}^{2/3})$, J can be taken to be a constant such as 1. In the following analysis, we consider the specific case when

$$J = 1 \text{ (or } \bar{n}_J = \tilde{n}) \text{ and } \bar{n}_K = O(\tilde{n}^{1/3}).$$

When either the microstructure error or the asynchronicity exists, the realized covariance is seriously biased. An asymptotic normality result in Zhang (2009) reveals that TSCV can simultaneously remove the bias due to the microstructure error and the bias due to the asynchronicity. However, this result is not adequate for our application to the vast volatility matrix estimation. The maximum componentwise estimation error a_p depends on the number of assets p . To understand its impact on a_p , we need to establish the concentration inequality. In particular, for a sufficiently large $|x| = O((\log p)^a)$, if

$$\max_{i,j} P\{\sqrt{n}|\sigma_{ij} - \hat{\sigma}_{ij}| > x\} < \exp(-Cx^{1/a}), \quad (17)$$

for two positive constants a and C , then

$$a_p = |\Sigma - \hat{\Sigma}|_\infty = O_P\left(\frac{(\log p)^a}{\sqrt{n}}\right). \quad (18)$$

We will show in the next section that the result indeed holds with $a = 1/2$ and n replaced by the minimum subsample size. Hence the impact of the number of assets is limited, only of the logarithmic order.

3.3 Concentration Inequalities

Inequality (17) requires the conditions on both diagonal elements and off-diagonal elements. Technically, they are treated differently. For the diagonal cases, the problem corresponds to the estimation of integrated volatility and there is no issue of asynchronicity. TSCV (16) reduces to TSRV (Zhang, *et al.*, 2005), which is explicitly given by

$$\widehat{\langle X, X \rangle}_1 = [X^o, X^o]_1^{(K)} - \frac{\bar{n}_K}{\bar{n}_J} [X^o, X^o]_1^{(J)}, \quad (19)$$

where

$$[X^o, X^o]_1^{(K)} = \frac{1}{K} \sum_{i=K}^n (X_{t_i}^o - X_{t_{i-K}}^o)^2$$

and $\bar{n}_K = (n - K + 1)/K$.

As shown in Zhang, *et al.* (2005), the optimal choice of K has order $K = O(n^{2/3})$ and J can be taken to be a constant such as 1. Again, for the TSRV, in the following analysis, we will consider the specific case when $J = 1$ (or $\bar{n}_J = n$) and $\bar{n}_K = O(n^{1/3})$.

To facilitate the reading, we relegate the technical conditions and proofs to the appendix. The following two results establish the concentration inequalities for the integrated volatility and integrated covariation.

Theorem 1. *Let X process be as in (13), and n be the total number of observations for the X process during the time interval $(0, 1]$. Under Conditions 1-4 in section A.1, for $x \in [0, cn^{1/6}]$,*

$$P\left\{n^{1/6}|\widehat{\langle X, X \rangle}_1 - \int_0^1 \sigma_t^{(X)^2} dt| > x\right\} \leq 4 \exp\{-Cx^2\}$$

for positive constants c and C . A set of candidate values for c and C are given in (49) for the case when the TSRV parameters are chosen according to Condition 5.

Theorem 2. *Let X and Y processes be as in (13), and \tilde{n} be the total number of refresh times for the processes X and Y during time interval $(0, 1]$. Under Conditions 1-5 in section A.1, for $x \in [0, c\tilde{n}^{1/6}]$,*

$$P\{\tilde{n}^{1/6}|\widehat{\langle X, Y \rangle}_1 - \int_0^1 \sigma_t^{(X)} \sigma_t^{(Y)} \rho_t^{(X,Y)} dt| > x\} \leq 8 \exp\{-Cx^2\}$$

for positive constants c and C . A set of candidate values for c and C are given in (52) for the case when the TSCV parameters are chosen according to Condition 5.

3.4 Error rates on risk approximations

Having had the above concentration inequalities, we can now readily give an upper bound of the risk approximations. Consider the p log-price processes as in Section 2.1. Suppose the processes are observed with the market microstructure noises. Let $\tilde{n}^{(i,j)}$ be the observation frequency obtained by the pairwise-refresh method for two processes $X^{(i)}$ and $X^{(j)}$ and \tilde{n}_* be the observation frequency obtained by the all-refresh method. Clearly, $\tilde{n}^{(i,j)}$ is typically much larger than \tilde{n}_* . Hence, most elements are estimated more accurately using the pairwise-refresh method than using the all-refresh method. On the other hand, for less liquidly traded pairs, its observation frequency of pairwise-refresh time can not be an order of magnitude larger than \tilde{n}_* .

Using (18), an application to Theorems 1 and 2 to each element in the estimated integrated covariance matrix yields

$$a_p^{\text{pairwise-refresh}} = |\hat{\Sigma}^{\text{pairwise}} - \Sigma|_{\infty} = O_P \left(\frac{\sqrt{\log p}}{\tilde{n}_{\min}^{1/6}} \right), \quad (20)$$

where $\tilde{n}_{\min} = \min_{i,j} \tilde{n}^{(i,j)}$ be the minimum number of observations of the pairwise-refresh time.

Note that based on our proofs which don't rely on particular properties of pairwise-refresh times, our results of Theorem 1 and Theorem 2 are applicable to all-refresh method as well, with the observation frequency of the pairwise-refresh times replaced by that of the all-refresh times. Hence, using the all-refresh time scheme, we have

$$a_p^{\text{all-refresh}} = |\hat{\Sigma}^{\text{all-refresh}} - \Sigma|_{\infty} = O_P \left(\frac{\sqrt{\log p}}{\tilde{n}_*^{1/6}} \right). \quad (21)$$

Clearly, \tilde{n}_{\min} is larger than \tilde{n}_* . See Figure 2. Hence, the pairwise refresh method gives a somewhat more accurate estimate in terms of the maximum elementwise estimation error.

3.5 Projections of estimated volatility matrices

The risk approximations (9)-(11) hold for any solutions to (8) whether the matrix $\hat{\Sigma}$ is positive semi-definite or not. However, convex optimization algorithms typically require the positive semi-definiteness of the matrix $\hat{\Sigma}$. Yet, the estimates based on the elementwise estimation sometimes can not satisfy this and even the one from all-refresh method can have the same problem if TSRV is used. This leads to the issue of how to project a symmetric matrix onto the space of positive semi-definite matrices.

There are two intuitive methods for projecting a $p \times p$ symmetric matrix \mathbf{A} onto the space of positive semi-definite matrices. Consider the singular value decomposition: $\mathbf{A} = \mathbf{\Gamma}^T \text{diag}(\lambda_1, \dots, \lambda_p) \mathbf{\Gamma}$,

where $\mathbf{\Gamma}$ is an orthogonal matrix, consisting of p eigenvectors. The two intuitive appealing projection methods are

$$\mathbf{A}_1^+ = \mathbf{\Gamma}^T \text{diag}(\lambda_1^+, \dots, \lambda_n^+) \mathbf{\Gamma}, \quad (22)$$

where λ_j^+ is the positive part of λ_j and

$$\mathbf{A}_2^+ = (\mathbf{A} + \lambda_{\min}^- I_p) / (1 + \lambda_{\min}^-), \quad (23)$$

where λ_{\min}^- is the negative part of the minimum eigenvalue. For both projection methods, the eigenvectors remain the same as those of \mathbf{A} . When \mathbf{A} is positive semi-definite matrix, we have obviously that $\mathbf{A}_1 = \mathbf{A}_2 = \mathbf{A}$.

In applications, we apply the above transformations to the estimated correlation matrix \mathbf{A} rather than directly to the volatility matrix estimate $\hat{\Sigma}$. The correlation matrix \mathbf{A} has diagonal elements of 1. The resulting matrix under the projection method (23) apparently still satisfies this property, whereas the one under the projection method (22) does not. As a result, the projection method (23) keeps the integrated volatility of each asset intact.

In the simulation and empirical studies, we applied both projections. It turns out that there is no significant difference between the two projection methods in terms of result. We decided to apply only the projection (23) in all numerical studies, as it keeps the individual volatility estimate intact.

3.6 Comparisons between pairwise-refresh and all-refresh methods

The pairwise-refresh method keeps far richer information in the high-frequency data than the all-refresh method. See Figure 2. Thus, it is expected to estimate each element more precisely. Yet, the estimated correlation matrix is typically not positive semi-definite. As a result, projection (23) can distort the accuracy of elementwise estimation. On the other hand, the all-refresh method is typically positive semi-definite or nearly so. The property (12) typically entails the positive semi-definiteness property, as long as the volatility estimator for $\langle X, X \rangle$ is always nonnegative. For example, using the realized kernel method as the building block, the positive semi-definite version can easily be obtained. Therefore, the projection (23) has less impact on the all-refresh method than on the pairwise-refresh method.

Risk approximations (9)–(11) are only the upper bounds. The upper bounds are controlled by a_p , which has rates of convergence govern by (20) and (21). While the average number of observations of pairwise-refresh time is far larger than the number of observations \tilde{n}_* of the all-refresh time, the minimum number of observations of pairwise-refresh time \tilde{n}_{\min} is not much larger than \tilde{n}_* . Therefore, the upper bounds (20) and (21) are approximately of the same order. This together with the distortion due to projection do not leave much advantage for the pairwise-refresh

method.

4 Simulation Studies

In this section, we simulate the market trading data using a reasonable stochastic model. As the latent prices and dynamics of simulations are known, our study on the risk profile is facilitated. It is a good tool to verify our theoretical results and to quantify the finite sample behaviors. In particular, we would like to demonstrate that high frequency data based approaches have a better risk profile than those based on the low frequency data.

Throughout this paper, the risk is referring to the standard deviation of portfolio's returns. To avoid ambiguity, we call $\sqrt{R(\mathbf{w}_{opt})}$ the theoretical optimal risk or oracle risk, $\sqrt{R_n(\hat{\mathbf{w}}_{opt})}$ the perceived optimal risk, and $\sqrt{R(\hat{\mathbf{w}}_{opt})}$ the actual risk of the perceived optimal allocation.

4.1 Design of Simulations

A slightly modified version of the simulation model in Barndorff-Nielsen *et al.* (2008) is used to generate the latent price processes of p traded assets. It is a multivariate factor model with stochastic volatilities. Specifically, the latent log-prices $X_t^{(i)}$ follow

$$dX_t^{(i)} = \mu^{(i)}dt + \rho^{(i)}\sigma_t^{(i)}dB_t^{(i)} + \sqrt{1 - (\rho^{(i)})^2}\sigma_t^{(i)}dW_t + \lambda^{(i)}dZ_t, \quad i = 1, \dots, p, \quad (24)$$

where the elements of B , W and Z are independent standard Brownian motions. The spot volatility obeys the independent Ornstein-Uhlenbeck processes:

$$d\varrho_t^{(i)} = \alpha^{(i)}(\beta_0^{(i)} - \varrho_t^{(i)})dt + \beta_1^{(i)}dU_t^{(i)}, \quad (25)$$

where $\varrho_t^{(i)} = \log \sigma_t^{(i)}$ and $U_t^{(i)}$ is an independent Brownian motion. The stationary distribution is given by $N(\beta_0^{(i)}, [\beta_1^{(i)}]^2/(2\alpha^{(i)}))$. The integrated quadratic variation and covariation are given by

$$\begin{aligned} \langle X^{(i)} \rangle_t &= \int_0^t (\sigma_s^{(i)})^2 ds + \lambda^{(i)}t, \\ \langle X^{(i)}, X^{(j)} \rangle_t &= \int_0^t \sqrt{1 - (\rho_s^{(i)})^2} \sqrt{1 - (\rho_s^{(j)})^2} \sigma_s^{(i)} \sigma_s^{(j)} ds. \end{aligned}$$

The analytic formula for the conditional covariance matrix $\Sigma_{t,\tau}$ in (3) can be found for our model, but we decide not to report it for brevity.

The number of assets p is taken to be 50. Slightly modified from Barndorff-Nielsen *et al.* (2008), the parameters is set to be $(\mu^{(i)}, \beta_0^{(i)}, \beta_1^{(i)}, \alpha^{(i)}, \rho^{(i)}) = (0.03x_1^{(i)}, -x_2^{(i)}, 0.75x_3^{(i)}, -1/40x_4^{(i)}, -0.7)$

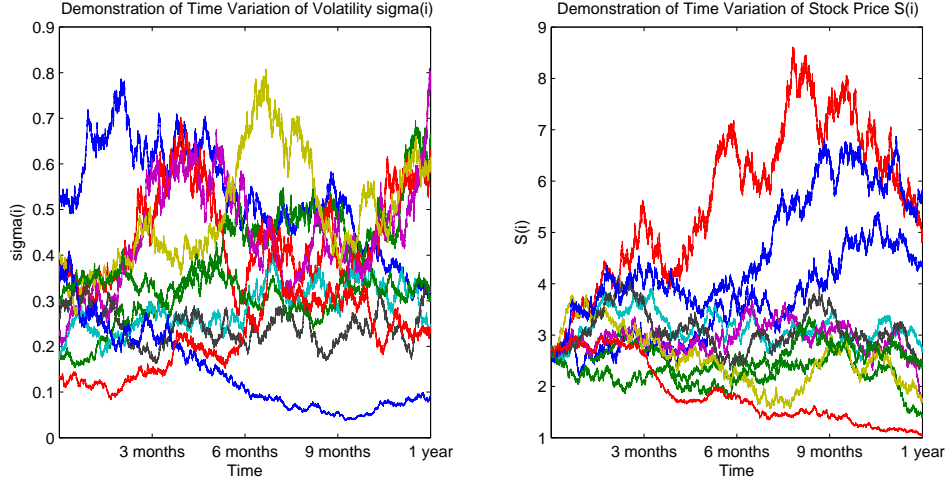


Figure 1: The volatility and asset price processes of 10 simulated assets.

where $x_j^{(i)}$ is an independent realization from the uniform distribution on $[0.7, 1.3]$. The parameters are kept fixed during the simulations. In addition, $\lambda^{(i)} = \exp(\beta_0^{(i)})$, which makes the volatility matrix well conditioned.

The model (24) is used to generate the latent log-price values with initial values $X_0^{(i)} = 1$ (log-price) and $\varrho_0^{(i)}$ from its stationary distribution. The Euler scheme is used to generate latent price at the frequency of once per second. To account for the market microstructure noise, the Gaussian noises $\varepsilon_t^{(i)} \sim N(0, \omega^2)$ with $\omega = 0.0005$ are added. Therefore, like (14), the observed log-prices are $X_t^{o(i)} = X_t^{(i)} + \varepsilon_t^{(i)}$. To gain a sense of the extent to which the asset volatilities $\sigma_t^{(i)}$ and prices $P_t^{(i)} (= \exp(X_t^{o(i)}))$ vary through time, we plot demonstrative graphs of 10 assets' volatility and price processes over a year in Figure 1.

To model the non-synchronicity, p independent Poisson processes with intensive parameters $\lambda_1, \lambda_2, \dots, \lambda_p$ are used to simulate the trading times of the assets. Motivated by the US equity trading dataset (the total number of seconds in a common trading day of the US equity is 23400), we set the trading intensity parameters λ_i 's to be $0.02i \times 23400$ for $i = 1, 2, \dots, 50$, meaning that the average numbers of trading times for each asset are spread out in the arithmetic sequence of the interval $[468, 23400]$.

4.2 An oracle investment strategy and risk assessment

An oracle investment strategy is usually a decent benchmark for other portfolio strategies to be compared with. There are several oracle strategies. The one we choose is to make portfolio allocation based on the covariance matrix estimated using latent prices at the finest grid (one per second). Latent prices are the noise-free prices of each asset at every time points (one per second),

which are unobservable in practice and is available to us only in the simulation. Therefore, for each asset, there are 23400 latent prices in a normal trading day. We will refer to the investment strategy based on the latent prices as the oracle or latent strategy. This strategy is not available for the empirical studies.

The assessment of risk is based on the high-frequency data. For a given portfolio strategy, its risk is computed based on the latent prices at the finest grid (one per second) for the in-the-sample simulation studies; its risk is computed based on the latent prices at every 15 minutes for the out-of-sample simulation studies; whereas for the empirical studies, the observed prices at every 15 minutes are used to assess its risk. This mitigates the influence of the microstructure noises. For the empirical study, we do not hold positions overnight therefore are immune to the overnight price jumps (we will discuss the details in Section 5).

4.3 In-sample Risk Approximation and Optimal Allocation

Based on the past $h = 1$ day, the latent prices (at the finest grid) based estimated TSCV covariance matrix (called latent covariance for short) is regarded as the true covariance matrix. There are several methods for estimating covariance matrix based on observed non-synchronized high-frequency data with microstructure noise. In particular, we employ all-refresh method based TSCV covariance matrix (called all-refresh TSCV covariance), all-refresh method based realized kernel covariance matrix (called all-refresh RK covariance, for short), and pairwise-refresh method based TSCV covariance matrix (called pairwise-refresh TSCV covariance). The all-refresh RK covariance is included since it is positive semi-definite and there is no distortion effect due to projection. The latent covariance serves as the oracle covariance matrix from which the actual portfolio risk of any portfolio is computed. The conditioning number of the latent covariance of the $p = 50$ assets ranges from 192.27 to 226.46, with median 210.34, across 100 simulations. The medians of the minimum and maximum eigenvalues are respectively 0.0004 and 0.0838. For the all-refresh RK approach, the bandwidth of the realized kernel H is chosen to be 1, which gives the best risk profile in our numerical analysis.

The efficiencies of using the rich high-frequency data between pairwise-refresh and all-refresh methods are contrasted. In particular, for each realization, we compute the median number of pairwise-refresh times $\text{median}_{i,j}(\tilde{n}^{(i,j)})$, the minimum number of pairwise-refresh times $M_{\min} = \min_{i,j}(\tilde{n}^{(i,j)})$ (see (20)), and the number of all-refresh times \tilde{n}_* (see (21)). The distributions of these three numbers are summarized in Figure 2. It is clear that the pairwise refresh scheme uses far more data on average, yet minimum number of pairwise-refresh time is not appreciably larger than that of refresh time.

To gain insights on the risk approximations, we consider 4 specific portfolios of the $p = 50$ assets

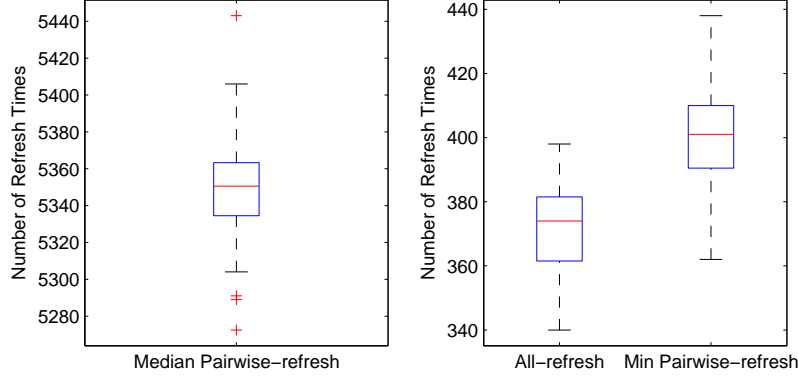


Figure 2: The distributions (from left to right) of the median number of pairwise-refresh times, the minimum number of pairwise-refresh times, and the number of all-refresh times per day across 100 simulations.

with the weight vectors

$$\begin{aligned} w_1 &= \left(\frac{1}{p}, \frac{1}{p}, \dots, \frac{1}{p}\right)^T, & w_2 &= (1, 0, \dots, 0)^T, \\ w_3 &= \left(\frac{b}{2} - \frac{1}{2} + \frac{2}{p}, \frac{1}{2} - \frac{b}{2}, \frac{1}{p}, \dots, \frac{1}{p}\right)^T, & w_4 &= \left(\frac{1}{2} + \frac{b}{2}, \frac{1}{2} - \frac{b}{2}, 0, \dots, 0\right)^T \end{aligned}$$

with $b = 3$. Their daily risks are computed based on various covariance estimators and are compared with the actual risk, which is computed based on the latent price. This is done across 100 simulations. The medians, robust standard deviation (defined as interquartile range divided by 1.35) and other characteristics are summarized in Table 1.

From the result, we can see that both the all-refresh TSRV and pairwise-refresh TSRV methods, especially all-refresh TSRV method, have a tendency to underestimate the risk in comparison with the latent risks, while all-refresh RK method has a tendency to overestimate the risk. In terms of the absolute risk difference from the oracle, for 3 out of the 4 portfolios, pairwise-refresh TSRV method outperforms the all-refresh TSRV method. The same relationship can be observed when we turn to the L_1 norm of the absolute covariance difference (a_p) as well. The RK method outperforms the TSRV method. These are in line with our expectation.

We now study the problem of the optimal portfolio allocation under gross exposure constraints. The optimal allocation vectors are computed based on the latent covariance, all-refresh TSCV covariance, all-refresh RK covariance and pairwise-refresh TSCV covariance and their actual risks are computed based on the latent covariance matrix. The medians of these actual risks against the gross exposure parameter c are depicted in Figure 3.

Firstly, the all-refresh RK method outperforms the two TSRV methods when the gross exposure is below 3.7. The pairwise-refresh TSRV method outperforms the all-refresh TSRV method where the gross exposure is smaller than 1.2. That agrees with what we expected since the smaller the

Table 1: **Risk approximation for $p = 50$ and $n = 100$**

We used the high frequency data for 100 independent trading days. The covariance of the 50 stocks is estimated according to various estimators. These estimated covariance matrices are used to compute the perceived risks of 4 portfolios. Relevant statistics are recorded. (All the characteristics are annualized.)

<i>Median and Robust Standard Deviation (RSD) of Risk</i>				
Portfolio	Latent Median(RSD)	All-refresh TSRV Median(RSD)	All-refresh RK Median(RSD)	Pairwise TSRV Median(RSD)
w_1	0.4408 (0.0032)	0.3875 (0.1075)	0.4343 (0.0241)	0.4192 (0.0690)
w_2	0.5916 (0.0060)	0.5229 (0.1259)	0.6230 (0.0258)	0.5936 (0.1285)
w_3	0.5399 (0.0044)	0.4694 (0.0907)	0.5833 (0.0255)	0.5202 (0.0736)
w_4	0.8442 (0.0077)	0.7531 (0.1748)	0.9228 (0.0418)	0.8390 (0.1789)
<i>Median and RSD of Absolute Risk Difference from the Oracle (Latent)</i>				
Portfolio	All-refresh TSRV Median(RSD)	All-refresh RK Median(RSD)	Pairwise TSRV Median(RSD)	
w_1	0.0889 (0.0769)	0.0183 (0.0153)	0.0547 (0.0439)	
w_2	0.1054 (0.0700)	0.0344 (0.0272)	0.0804 (0.0813)	
w_3	0.0936 (0.0665)	0.0437 (0.0300)	0.0599 (0.0593)	
w_4	0.1470 (0.1022)	0.0794 (0.0393)	0.1089 (0.0941)	
<i>Median and RSD of L_1 Norm of Absolute Covariance Difference (a_p)</i>				
Portfolio	All-refresh TSRV Median(RSD)	All-refresh RK Median(RSD)	Pairwise TSRV Median(RSD)	
	0.2476 (0.1460)	0.0603 (0.0270)	0.1730 (0.0746)	

gross exposure is, the tighter the bound (9) on the risk difference. It is obvious that the pairwise-refresh TSRV method gives an estimated covariance matrix with higher element-wise accuracy than the all-refresh TSRV method, therefore the former outperforms the latter where the bound is the tightest (gross exposure below 1.2) for this simulation design.

Secondly, all the methods produce an upward-sloping risk curve up to some point and an almost flat curve beyond that (the curve is clipped). This is mainly due to the fact that we use only the intra-day data for 1 trading day, which does not result in sufficient amount of data to yield a stable estimate of the 50×50 covariance matrix. As the result, the estimated covariance matrix can be ill-conditioned. As c increases, the selected portfolios become increasingly unstable. When c reaches 5 or so, the selected portfolio becomes basically a randomly selected portfolio. Hence, their actual risks become larger and flat afterwards.

4.4 Out-of-sample Optimal Allocation

One of the main purposes of this paper is to investigate the comparative advantage of the high frequency based methods against the low frequency based method (especially in the context of portfolio investment). Hence, it is essential for us to run the following out-of-sample investment strategy test which includes both the high frequency and low frequency based approaches. Moreover, since in the empirical studies, we do not know the latent asset prices, the out-of-sample test

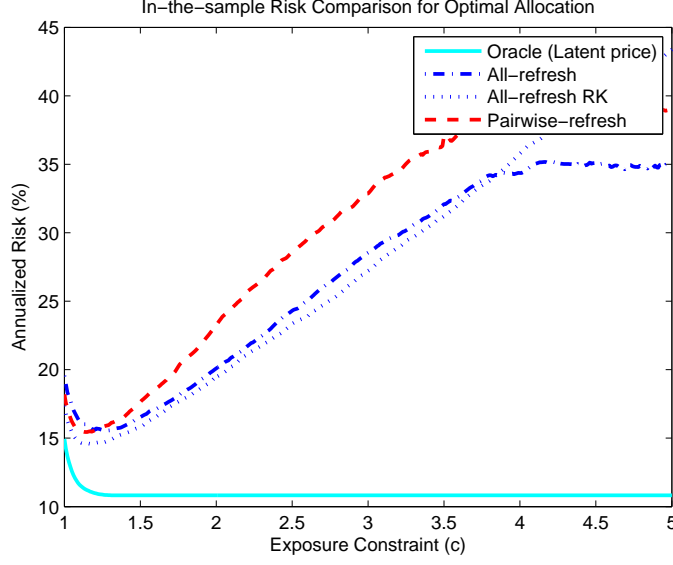


Figure 3: The medians of the actual risks of the in-sample optimal allocations based on the high-frequency estimated covariance matrices using 1 trading day’s intra-day data($p = 50$, $n = 100$).

should be designed so that it can also be conducted in the empirical studies.

We simulate the prices of 50 traded assets using the model (24) and (25) with microstructure noise for the duration of 200 trading days (numbered as day 1, day 2, ..., day 200) and record all the tick-by-tick trading times and trading prices of the assets. We assume that there are no overnight jumps for asset prices, meaning one trading day’s closing price of an asset is always the same as the next trading day’s opening price of that asset.

We start investing 1 unit of capital into the pool of assets with low frequency and high frequency based strategies from day 101 (the portfolios are bought at the opening of day 101). For the low frequency strategy, we use the previous 100 trading days’ daily closing prices to compute the sample covariance matrix and make the portfolio allocation accordingly with the gross exposure constraints. For the all-refresh high frequency strategies, we use the previous $h = 10$ trading days’ tick-by-tick trading data, use all-refresh time to synchronize the trades of the assets before applying realized kernel and TSCV to estimate the integrated volatility matrix and make the portfolio allocation, while for the pairwise-refresh high frequency strategy, we use pairwise-refresh times to synchronize each pair of assets and apply TSCV to estimate the integrated covariance for the corresponding pair. With the projection technique (23), the resulting TSCV integrated volatility matrix can always be transformed to a positive semi-definite matrix which facilitates the optimization.

We run two investment strategies. In the first strategy, the portfolio is held for $\tau = 1$ trading day before we re-estimate the covariation structure and adjust the portfolio weights accordingly. The second strategy is the same as the first one except for the fact that the portfolio is held for

$\tau = 5$ trading days before rebalance.

In the investment horizon (which is from day 101 to day 200 in this case), we record the 15-minute portfolio returns based on the latent prices of the assets, the variation of the portfolio weights across 50 assets, and other relevant characteristics. While it appears that 100 trading days is short, calculating 15-minute returns increases the size of the relevant data for computing the risk by a factor of 26.

We study those portfolio features for a whole range of gross exposure constraint c from $c = 1$, which stands for the no-short-sale portfolio strategy, to $c = 3$. This is usually the relevant range of gross exposure for investment purpose.

The standard deviations and other characteristics of the strategy for $\tau = 1$ are presented in Table 2 (the case $\tau = 5$ is very similar, therefore omitted). The standard deviations represent the actual risks of the strategy. As we only optimize the risk profile, we should not look significantly on the returns of the optimal portfolios. They can not even be estimated accurately with such a short investment horizon. Figures 4 and 5 provides graphical details to these characteristics for both $\tau = 1$ and $\tau = 5$.

Table 2: **The out-of-sample performance of daily-rebalanced optimal portfolios with gross-exposure constraint**

We simulate one trial of intra-day trading data for 50 assets, make portfolio allocations for 100 trading days and rebalance daily. The standard deviations and other characteristics of these portfolios are recorded. All the characteristics are annualized (Max Weight: Median of maximum weights; Min Weight: Median of minimum weights; No. of Long: Median of numbers of long positions whose weights exceed 0.001; No. of Short: Median of numbers of short positions whose absolute weights exceed 0.001)

Methods	Std Dev %	Max Weight	Min Weight	No. of Long	No. of Short
<i>Low Frequency Sample Covariance Matrix Estimator</i>					
$c = 1$ (No short)	16.69	0.19	-0.00	13	0
$c = 2$	16.44	0.14	-0.05	28.5	20
$c = 3$	16.45	0.14	-0.05	28.5	20
<i>High Frequency All-Refresh TSRV Covariance Matrix Estimator</i>					
$c = 1$ (No short)	16.08	0.20	-0.00	15	0
$c = 2$	14.44	0.14	-0.05	30	19
$c = 3$	14.44	0.14	-0.05	30	19
<i>High Frequency All-Refresh RK Covariance Matrix Estimator</i>					
$c = 1$ (No short)	17.20	0.22	-0.00	12.5	0
$c = 2$	20.35	0.22	-0.09	22	18
$c = 3$	31.37	0.34	-0.19	23.5	23
<i>High Frequency Pairwise-Refresh TSRV Covariance Matrix Estimator</i>					
$c = 1$ (No short)	15.34	0.18	-0.00	15	0
$c = 2$	12.72	0.13	-0.03	31	18
$c = 3$	12.72	0.13	-0.03	31	18

For both holding lengths $\tau = 1$ and $\tau = 5$, the all-refresh TSRV and pairwise-refresh TSRV

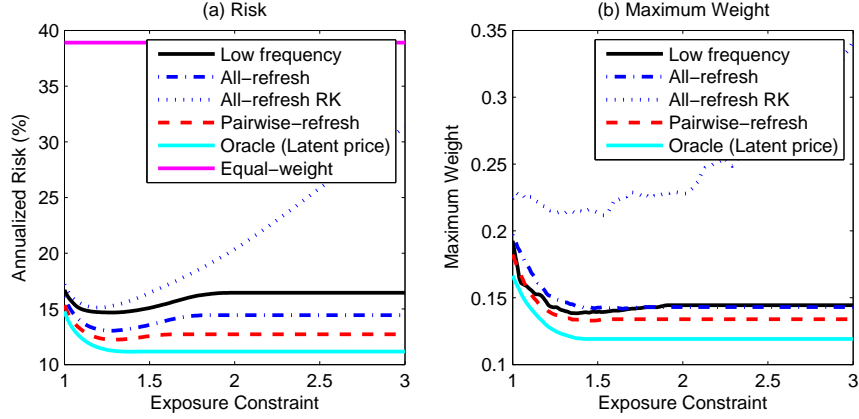


Figure 4: Out-of-sample performance of daily-rebalanced optimal portfolios based on high-frequency and low-frequency estimation of the integrated covariance matrix. (a) Annualized risk of portfolios. (b) Maximum weight of allocations.

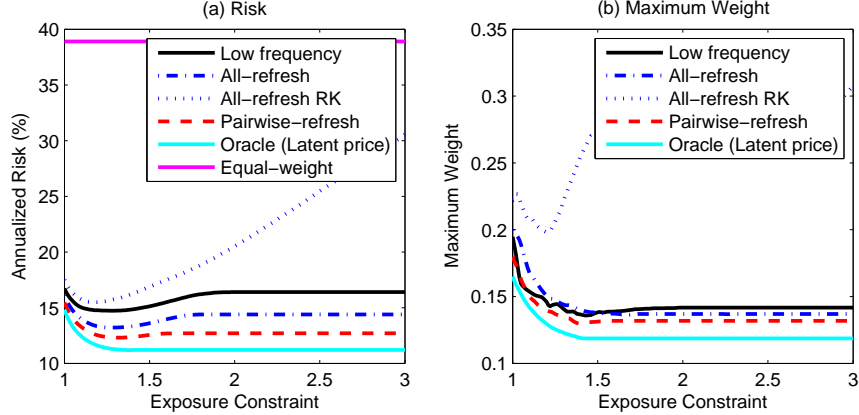


Figure 5: Out-of-sample performance of optimal portfolios based on high-frequency and low-frequency estimation of the integrated covariance matrix with holding period $\tau = 5$.

approaches outperform significantly the low frequency one in terms of risk profile for the whole range of the gross exposure constraint. This supports our theoretical results and intuitions. The shorter estimation window allows these 2 high frequency approaches to deliver consistently better results than the low frequency one. The low-frequency strategy outperforms significantly the equal-weight portfolio (see Figure 4 and Figure 5). Slightly surprising is the fact that the low frequency approach also outperforms the all-refresh RK approach. We believe it must be due to the instability of the estimated realized kernel covariance matrix.

All the risk curves attain their minimum around $c = 1.2$ (see Figure 4 and Figure 5), which falls into our expectation again, since that must be the point where the marginal increase in estimation error outpaces the marginal decrease in specification error. This, coupled with the result we get in the empirical studies section, will give us some guidelines about what gross exposure constraint to

use in investment practice.

Firstly, the pairwise method outperforms the all-refresh method, as expected. Secondly, the risk of the low frequency approach only increases at a mild speed as the gross exposure constraint increases. A possible explanation is that only 50 assets is considered, therefore the estimation error accumulation effect is not dominating as badly as we were afraid it would be, given the low frequency covariance sampling window is the previous 100 trading days. Another possible reason could be that as the data is generated by a stationary stochastic model, the low frequency approach may be able to capture some of the stationarity within the model.

In terms of portfolio weights, neither the low frequency nor the high frequency optimal no-short-sale portfolios are well diversified with all approaches assigning a concentrated weight of around 20% to one individual asset. Their portfolio risks can be improved by relaxing the gross-exposure constraint (Figure 4 and Figure 5).

5 Empirical Studies

The risk minimization problem (6) has important applications in asset allocation. We demonstrate its application in the stock portfolio investment in the 30 Dow Jones Industrial Average (DJIA) constituent stocks (will be called the 30 DJIA stocks for short).

The Dow Jones Industrial Average is one of the several stock market indices created by Charles Dow, the editor of Wall Street Journal and a co-founder of Dow Jones and Company. It is an index that shows how 30 large, publicly-owned companies based in the United States have traded during a standard trading session in the stock market. We make the portfolio allocation to the constituents of the index as of Sep 30, 2008 (The individual components of the DJIA are occasionally changed as market conditions warrant.)

To make asset allocation, we use the high frequency data of the 30 DJIA stocks from Jan 1, 2008 to September 30, 2008. These stocks are highly liquid. The intensity of trading for each given trading day is summarized by the maximum, minimum and median number of trades among these 30 stocks. The distributions of these summary statistics across those 9 months (189 trading days) are summarized in Figure 6. The period covers the birth of financial crisis in 2008.

At the end of each holding period of $\tau = 1$ or $\tau = 5$ trading days in the investment period (from May 27, 2008 to Sep 30, 2008), the covariance of the 30 stocks is estimated according to various estimators. They are the sample covariance of the last 100 trading days' daily return data (low-frequency), the all-refresh TSCV estimator of the last 10 trading days, the all-refresh RK estimator of the last 10 trading days (the bandwidth of the realized kernel H is chosen to be 1 since the risk profile for $H = 1$ outperforms other alternative choices of H), and the pairwise-refresh TSCV

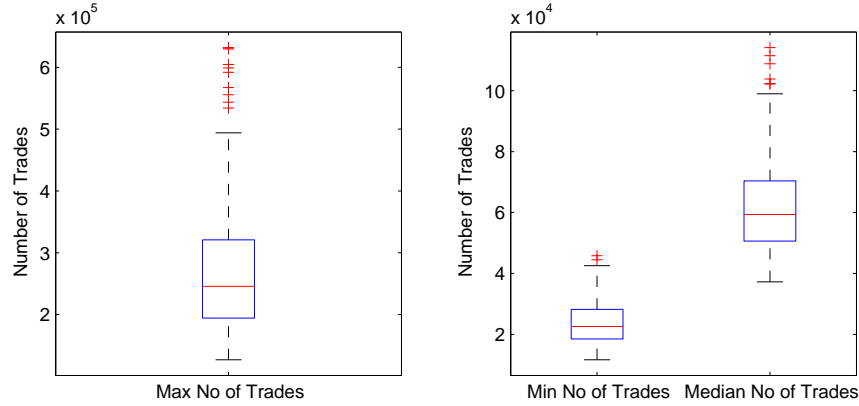


Figure 6: The distributions (from left to right) of the maximum, minimum and median number of trades of the 30 DJIA stocks per day, from Jan 02, 2008 to Sep 30, 2008 (189 trading days).

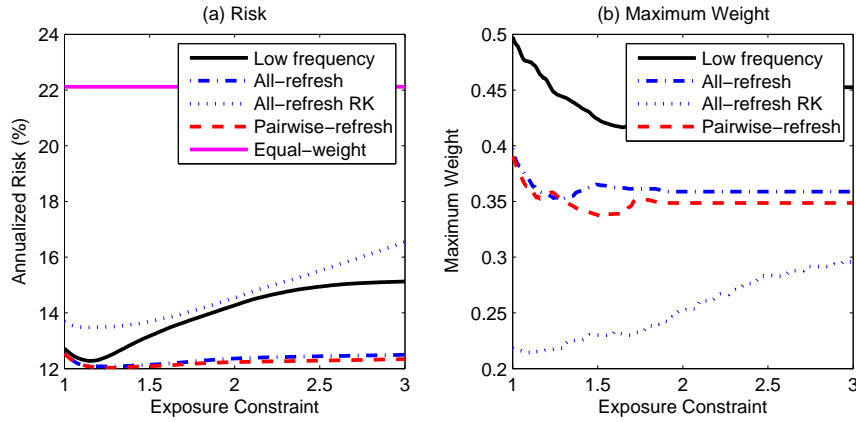


Figure 7: Out-of-sample performance of daily-rebalanced optimal portfolios for Dow Jones 30 constituent stocks with investment period from May 27, 2008 to Sep 30, 2008 (89 trading days). (a) Annualized risk of portfolios. (b) Maximum weight of allocations.

estimator of the last 10 trading days. These estimated covariance matrices are used to construct optimal portfolios with various exposure constraints. For $\tau = 5$, we do not count the overnight risks of the portfolio. The reason that the overnight price jumps are often due to the arrival of news and are irrelevant of the topic of our studies. The standard deviations and other characteristics of these portfolio returns for $\tau = 1$ are presented in Table 3 together with the characteristics of an equally weighted portfolio of the 30 DJIA stocks rebalanced daily. The standard deviations represent the actual risks. The risk is computed based on the 15 minutes returns. Figure 7 and Figure 8 provide the graphical details to these characteristics for both $\tau = 1$ and $\tau = 5$.

Table 3, Figures 7 and 8 reveal that in terms of the portfolio's actual risk, the all-refresh TSRV and pairwise-refresh TSRV strategies perform at least as well as the low frequency based strategy when the gross exposure is small and outperform the latter significantly when the gross exposure

Table 3: **The out-of-sample performance of daily-rebalanced optimal portfolios of the 30 DJIA stocks**

Methods	Std Dev %	Max Weight	Min Weight	No. of Long	No. of Short
<i>Low Frequency Sample Covariance Matrix Estimator</i>					
c = 1 (No short)	12.73	0.50	-0.00	8	0
c = 2	14.27	0.44	-0.12	16	10
c = 3	15.12	0.45	-0.18	18	12
<i>High Frequency All-Refresh TSCV Covariance Matrix Estimator</i>					
c = 1 (No short)	12.55	0.40	-0.00	8	0
c = 2	12.36	0.36	-0.10	17	12
c = 3	12.50	0.36	-0.10	17	12
<i>High Frequency All-Refresh RK Covariance Matrix Estimator</i>					
c = 1 (No short)	13.69	0.22	-0.00	14	0
c = 2	14.54	0.25	-0.15	17	10
c = 3	16.55	0.30	-0.23	17	11
<i>High Frequency Pairwise-Refresh TSCV Covariance Matrix Estimator</i>					
c = 1 (No short)	12.54	0.39	-0.00	9	0
c = 2	12.23	0.35	-0.08	17	12
c = 3	12.34	0.35	-0.08	17	12
<i>Unmanaged Index</i>					
Dow Jones 30 equally weighted	22.12				

is large. Both facts support our theoretical results and intuitions. Given 10 times the length of covariance estimation window, the low frequency approach still cannot perform better than the high frequency TSRV approaches, which affirms our belief that the high frequency TSRV approaches can significantly shorten the necessary covariance estimation window and capture better the short-term time-varying covariation structure (or the “local” covariance). These results, together with the ones presented in the simulation section, lend strong support to the above statement.

Again the fact that the all-refresh RK strategy is outperformed by the low frequency strategy could be due to the instability of the estimated realized kernel covariance matrix.

As the gross exposure constraint increases, the portfolio risk of the low frequency approach increases drastically relative to the ones of the high frequency TSRV approaches. The reason could be a combination of the fact that the low frequency approach does not produce a well-conditioned estimated covariance due to the lack of data and the fact that the low frequency approach can only attain the long run covariation but cannot capture well the “local” covariance dynamics. The portfolio risk of the high frequency TSRV approaches increased only moderately as the gross exposure constraint increases. From financial practitioner’s standpoint, that is also one of the comparative advantages of high frequency TSRV approaches, which means that investors do not need to be much concerned about the choice of the gross exposure constraint while using the high frequency TSRV approaches.

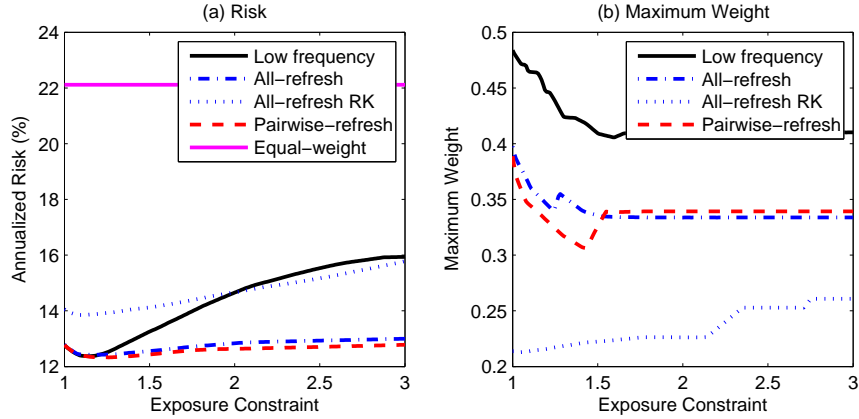


Figure 8: Out-of-sample performance of 5-day-rebalanced optimal portfolios for Dow Jones 30 constituent stocks with investment period from May 27, 2008 to Sep 30, 2008 (89 trading days). (a) Annualized risk of portfolios. (b) Maximum weight of allocations.

It can be seen that both the low frequency and high frequency optimal no-short-sale portfolios are not diversified enough. Their risk profiles can be improved by relaxing the gross-exposure constraint to around $c = 1.2$, i.e. 10% short positions and 110% long positions are allowed. The no-short-sale portfolios under all approaches have the maximum portfolio weight of 22% to 50%. As the gross exposure constraint relaxes, the pairwise-refresh TSRV approach has its maximum weight reaching the smallest value around 30% to 34% while the low frequency approach goes down to only around 40%. That is another comparative advantage of the high frequency approach in practice as a portfolio with less weight concentration is always considered more preferable by most of the investors.

Another interesting fact is that the equally weighted daily-rebalanced portfolio of the 30 DJIA stocks carries an annualized return of only -10% while DJIA went down 13.5% during the same period (May 27, 2008 to Sep 30, 2008), giving an annualized return of -38.3% . The cause of the difference is that we intentionally avoided holding portfolios overnight, hence not affected by the overnight price jumps. In the turbulent financial market of May to September 2008, that means our portfolio strategies are not affected by the numerous sizeable downward jumps. Those jumps are mainly caused by the news of distressed economy and corporations. The moves could deviate far from what the previously held covariation structure dictates.

6 Conclusion

We advocate the portfolio selection with gross-exposure constraint (Fan *et al.*, 2008b). It is less sensitive to the error of covariance estimation and is immune to the noise accumulation. The out-of-sample portfolio performance depends on the expected volatility in the holding period. It is at

best approximated and the gross-exposure constraints help reducing the error accumulation in the approximations.

Two approaches are proposed for the use of high-frequency data to estimate the integrated covariance: “all-refresh” and “pairwise-refresh” methods. The latter retains far more data on average and hence estimates more precisely element by element. Yet, the pairwise-refresh estimates are typically not positive semi-definite and projections are needed for the convex optimization algorithms. The projection distorts somewhat the performance of the pairwise-refresh strategies.

The use of high frequency financial data increases significantly the available sample size for volatility estimation, and hence shortens the time window for estimation, adapts better to local covariations. Our theoretical observations are supported by the empirical studies and simulations, in which we demonstrate convincingly that the high-frequency based strategies outperform the low-frequency based one in general.

With the gross-exposure constraint, the impact of the size of the candidate pool for portfolio allocation is limited. We derive the concentration inequalities to demonstrate this theoretically. Simulation and empirical studies also lend further support to it.

A APPENDIX. Conditions and Proofs

A.1 Conditions

The following conditions are needed. For simplicity, we state the conditions for integrated covariation (Theorem 2). The conditions for integrated volatility (Theorem 1) are simply the ones with $Y = X$.

Condition 1. $\mu_t^{(X)} = \mu_t^{(Y)} = 0$.

Condition 2. $0 < \sigma_t^{(X)}, \sigma_t^{(Y)} \leq C_\sigma < \infty, \forall t \in [0, 1]$.

Condition 3. The observation times are independent with the X and Y processes. The synchronized observation times for the X and Y processes satisfy $\sup_{1 \leq j \leq \tilde{n}} \tilde{n} \cdot (v_j - v_{j-1}) \leq C_\Delta \leq \infty$, where \tilde{n} is the observation frequency and $\mathcal{V} = \{v_0, v_1, \dots, v_{\tilde{n}}\}$ is the set of refresh times of the processes X and Y .

Condition 4. For the TSCV parameters, we consider the case when $J = 1$ ($\bar{n}_J = \tilde{n}$) and $\bar{n}_K = O(\tilde{n}^{1/3})$ such that

$$\frac{1}{2} \cdot \tilde{n}^{1/3} \leq \bar{n}_K \leq 2 \cdot \tilde{n}^{1/3}$$

Condition 5. The processes ϵ^X and ϵ^Y are independent.

Conditions 1 and 4 are imposed for simplicity. They can be removed at the expenses of lengthier proofs. For a short horizon and high-frequency, whether Condition 1 holds or not has little impact on the investment. For estimating integrated volatility, the synchronized time becomes observation time $\{\tau_{n,j}\}$ and Condition 3 and 5 becomes

$$\sup_{1 \leq j \leq n} n \cdot (\tau_{n,j} - \tau_{n,j-1}) \leq C_\Delta < \infty \quad (26)$$

and

$$\frac{1}{2} \cdot n^{1/3} \leq \bar{n}_K \leq 2 \cdot n^{1/3}.$$

A.2 Lemmas

We need the following three lemmas for the proof of Theorems 1 and 2. In particular, Lemma 2 is exponential type of inequality for any dependent random variables that have a finite moment generation function. It is useful for many statistical learning problems. Lemma 3 is a concentration inequality for the realized volatility based on discretely observed latent process.

Lemma 1. *When $Z \sim N(0, 1)$, for any $|\theta| \leq \frac{1}{4}$,*

$$E \exp\{\theta(Z^2 - 1)\} \leq \exp(2\theta^2).$$

Proof. Using the moment generating function of $Z^2 \sim \chi_1^2$, we have

$$E \exp\{\theta(Z^2 - 1)\} = \exp\left\{-\frac{1}{2} \log(1 - 2\theta) - \theta\right\}.$$

Let $g(x) = \log(1 - x) + x + x^2$ with $|x| \leq 1/2$. Then, $g'(x) = x(1 - 2x)/(1 - x)$ is nonnegative when $x \in [0, 1/2]$ and negative when $x \in [-1/2, 0]$. In other words, $g(x)$ has a minimum at point 0, namely $g(x) \geq 0$ for $|x| \leq 1/2$. Consequently, for $|\theta| \leq 1/4$,

$$\log(1 - 2\theta) \geq -2\theta - (2\theta)^2.$$

Hence,

$$E \exp\{\theta(Z^2 - 1)\} \leq \exp(2\theta^2).$$

Lemma 2. *For a set of random variables X_i , $i = 1, \dots, K$, if when $|\theta| \leq C_1$,*

$$E \exp(\theta X_i) \leq \exp(C_2 \theta^2), \quad (27)$$

for some two positive constants C_1 and C_2 , then

$$P\left\{\left|\sum_{i=1}^K w_i X_i\right| > x\right\} \leq 4 \exp\left(-\frac{x^2}{16C_2 w^2}\right), \text{ when } 0 \leq x \leq 2C_1 C_2,$$

where w_i 's are weights satisfying $\sum_{i=1}^K |w_i| \leq w \in [1, \infty)$.

Proof. By the Markov inequality, for $0 \leq \theta \leq C_1$, we have

$$P(|X_i| > x) \leq \exp(-\theta x) E \exp(\theta |X_i|) \leq 2 \exp(C_2 \theta^2 - \theta x). \quad (28)$$

Taking $\theta = x/(2C_2)$, we have

$$P\{|X_i| > x\} \leq 2 \exp\left(-\frac{x^2}{4C_2}\right), \quad \text{when } 0 \leq x \leq x_0, \quad (29)$$

where $x_0 = 2C_1 C_2$.

For a small constant $\xi > 0$ to be specified later, let

$$g_\xi(x) = \begin{cases} \exp(\xi x^2) & \text{when } 0 \leq x \leq x_0 \\ \exp(a_\xi + b_\xi x) & \text{when } x \geq x_0, \end{cases}$$

where $a_\xi = -\xi x_0^2$ and $b_\xi = 2\xi x_0$. Then $g_\xi(x)$ is a continuously differentiable increasing convex function on $[0, \infty)$. It follows from the Markov inequality and the convexity that, for $w^* = \sum_{i=1}^K |w_i|$

$$\begin{aligned} P\left(\left|\sum_{i=1}^K w_i X_i\right| > x\right) &\leq g_\xi(x)^{-1} E g_\xi\left(\left|\sum_{i=1}^K w_i X_i\right|\right) \\ &\leq g_\xi(x)^{-1} w^{*-1} \sum_{i=1}^K |w_i| E g_\xi(w |X_i|), \end{aligned} \quad (30)$$

which is further bounded by $4g_\xi(x)^{-1}$ if we can show that 4 is a common bound for $\{E g_\xi(w |X_i|)\}$.

Note that by (28) for $w b_\xi \leq \theta \leq C_1$,

$$\lim_{x \rightarrow \infty} g_\xi(x) \cdot P\{w |X_i| > x\} = 0.$$

It follows from the integration by parts that

$$\begin{aligned} E g_\xi(w |X_i|) &= 1 + \int_0^{x_0} 2\xi x \exp(\xi x^2) P(w |X_i| > x) dx \\ &\quad + \int_{x_0}^{\infty} b_\xi \exp(a_\xi + b_\xi x) P\{w |X_i| > x\} dx. \end{aligned} \quad (31)$$

By (29), the second term in (31) is bounded by

$$\int_0^{x_0} 2\xi x \exp(\xi x^2) 2 \exp(-C_3 x^2) dx = \frac{2\xi}{C_3 - \xi} \left(1 - \exp\{(\xi - C_3)x_0^2\}\right),$$

where $C_3 = (4C_2 w^2)^{-1}$. Using (28), the third term in (31) is bounded by

$$\begin{aligned} & 2b_\xi \exp(a_\xi) \int_{x_0}^{\infty} \exp(b_\xi x + C_2 \theta^2 - \theta w^{-1} x) dx \\ &= 2b_\xi \exp(a_\xi + C_2 \theta^2 + b_\xi x_0 - \theta w^{-1} x_0) / (\theta w^{-1} - b_\xi), \end{aligned}$$

provided that $w b_\xi < \theta \leq C_1$.

Choosing further θ to satisfy $a_\xi + C_2 \theta^2 + b_\xi x_0 - \theta w^{-1} x_0 \leq 0$ and $\xi \leq C_3$, it follows from the calculation in the previous paragraph that

$$E(g_\xi(w|X_i|)) \leq 1 + \frac{2\xi}{C_3 - \xi} + \frac{2b_\xi}{\theta w^{-1} - b_\xi}.$$

Taking $\theta = \theta_0 = \frac{C_1}{2w}$ and $\xi = \xi_0 = \frac{1}{16C_2 w^2}$, which satisfy the above conditions, it follows from direct calculation that

$$Eg_{\xi_0}(w|X_i|) \leq 1 + \frac{2\xi_0}{C_3 - \xi_0} + \frac{2b_{\xi_0}}{\theta_0 w^{-1} - b_{\xi_0}} = \frac{11}{3} < 4.$$

To summarize, from the above, we know that

$$Eg_{\xi_0}(w|X_i|) \leq 4 \text{ for all } i = 1, \dots, K.$$

Therefore, continued from (30), we have

$$P\left(\left|\sum_{i=1}^K w_i X_i\right| > x\right) \leq 4g_{\xi_0}(x)^{-1} = 4 \exp\left\{-\frac{x^2}{16C_2 w^2}\right\} \text{ when } 0 \leq x \leq 2C_1 C_2.$$

This completes the proof of the lemma.

Lemma 3. (A Concentration Inequality for Realized Volatility Based on Latent Process) *For a one dimensional process X_t following (1) that satisfies Conditions 1-2, when one observes X_t at times v_i , $i = 1, \dots, n$, and the observation frequency satisfies Condition 3 (see (26)), then, for $x \in [0, c\sqrt{n}]$,*

$$P\left\{n^{1/2}|\widetilde{[X, X]}_1 - \int_0^1 \sigma_t^2 dt| > x\right\} \leq 4 \exp\{-Cx^2\},$$

where $\widetilde{[X, X]}_1 = \sum_{i=1}^n (X_{v_i} - X_{v_{i-1}})^2$ is the realized volatility based on the discretely observed X process; the constants c and C can be taken as in (34).

Proof. Let $\tilde{X}_t = X_t - X_0 = \int_0^t \sigma_s dW_s$. By time-change for martingales, (see, for example, Theorem 4.6 of Karatzas and Shreve (2000)), if $\tau_t = \inf\{s : [\tilde{X}]_s \geq t\}$ where $[\tilde{X}]_s$ is the quadratic variation process, then $B_t := \tilde{X}_{\tau_t}$ is a Brownian-motion w.r.t. $\{\mathcal{F}_{\tau_t}\}_{0 \leq t \leq \infty}$. We then have that

$$E \exp\left(\theta(\tilde{X}_t^2 - \int_0^t \sigma_s^2 ds)\right) = E \exp(\theta(B_{[\tilde{X}]_t}^2 - [\tilde{X}]_t)).$$

Note further that for any t , $[\tilde{X}]_t$ is a stopping time w.r.t. $\{\mathcal{F}_{\tau_s}\}_{0 \leq s \leq \infty}$, and the process $\exp\left(\theta(B_s^2 - s)\right)$ is a sub-martingale for any θ . By the optional sampling theorem, using $[\tilde{X}]_u \leq C_\sigma^2 u$ (bounded stopping time), we have

$$E \exp\left(\theta(B_{[\tilde{X}]_u}^2 - [\tilde{X}]_u)\right) \leq E \exp\left(\theta(B_{C_\sigma^2 u}^2 - C_\sigma^2 u)\right).$$

Therefore, we have that, under Conditions 2 and 3,

$$\begin{aligned} & E\left(\exp\left\{\theta\sqrt{n}((\Delta X_i)^2 - \int_{v_{i-1}}^{v_i} \sigma_t^2 dt)\right\} \middle| \mathcal{F}_{v_{i-1}}\right) \\ & \leq E \exp\left\{\theta\sqrt{n}(B_{\frac{C_\sigma^2 C_\Delta}{n}}^2 - \frac{C_\sigma^2 C_\Delta}{n})\right\} \\ & = E \exp\left\{\theta \frac{C_\sigma^2 C_\Delta}{\sqrt{n}}(Z^2 - 1)\right\}, \end{aligned} \tag{32}$$

where $Z \sim N(0, 1)$ and $\Delta X_i = X_{v_i} - X_{v_{i-1}}$.

It follows from the law of iterated expectations and (32) that

$$\begin{aligned} & E \exp\left\{\theta\sqrt{n}(\widetilde{[X, X]}_1 - \int_0^1 \sigma_t^2 dt)\right\} \\ & = E(\exp\left\{\theta\sqrt{n}(\sum_{i=1}^{n-1} (\Delta X_i)^2 - \int_0^{v_{n-1}} \sigma_t^2 dt)\right\}) \\ & \quad \times E\left(\exp\left\{\theta\sqrt{n}(\Delta X_n^2 - \int_{v_{n-1}}^{v_n} \sigma_t^2 dt)\right\} \middle| \mathcal{F}_{v_{n-1}}\right) \\ & \leq E \exp\left\{\theta\sqrt{n}(\sum_{i=1}^{n-1} (\Delta X_i)^2 - \int_0^{v_{n-1}} \sigma_t^2 dt)\right\} E \exp\left\{\theta \frac{C_\sigma^2 C_\Delta}{\sqrt{n}}(Z^2 - 1)\right\}, \end{aligned}$$

where $Z \sim N(0, 1)$. Repeating the process above, we obtain

$$E \exp\left\{\theta\sqrt{n}(\widetilde{[X, X]}_1 - \int_0^1 \sigma_t^2 dt)\right\} \leq \left(E \exp\left\{\theta \frac{C_\sigma^2 C_\Delta}{\sqrt{n}}(Z^2 - 1)\right\}\right)^n.$$

By Lemma 1, we have for $|\theta| \leq \frac{\sqrt{n}}{4C_\sigma^2 C_\Delta}$,

$$E \exp\left\{\theta\sqrt{n}(\widetilde{[X, X]}_1 - \int_0^1 \sigma_t^2 dt)\right\} \leq \exp\{2\theta^2 C_\sigma^4 C_\Delta^2\}. \tag{33}$$

By Lemma 2, we have,

$$P\left\{n^{1/2}|\widetilde{[X, X]}_1 - \int_0^1 \sigma_t^2 dt| > x\right\} \leq 4 \exp\left\{-\frac{x^2}{32C_\sigma^4 C_\Delta^2}\right\}, \quad (34)$$

when $0 \leq x \leq C_\sigma^2 C_\Delta \sqrt{n}$.

A.3 Proof of Theorem 1

We first prove the results conditional on the set of observation times \mathcal{V} . Recall notation introduced in sections 3.2 and 3.3. Let n be the observation frequency. For simplicity of notation, without ambiguity, we will write $\tau_{n,i}$ as τ_i and $\sigma_t^{(X)}$ as σ_t . Denote the TSRV based on the unobserved latent process by

$$\widetilde{\langle X, X \rangle}_1^{(K)} = \widetilde{[X, X]}_1^{(K)} - \frac{\bar{n}_K}{\bar{n}_J} \widetilde{[X, X]}_1^{(J)}, \quad (35)$$

where $\widetilde{[X, X]}_1^{(K)} = K^{-1} \sum_{i=K}^n (X_{\tau_i} - X_{\tau_{i-K}})^2$. Then, from the definition, we have,

$$\begin{aligned} \widetilde{\langle X, X \rangle}_1 &= \widetilde{[X, X]}_1^{(K)} + \widetilde{[\epsilon^X, \epsilon^X]}_1^{(K)} + 2\widetilde{[X, \epsilon^X]}_1^{(K)} \\ &\quad - \frac{\bar{n}_K}{\bar{n}_J} \left(\widetilde{[X, X]}_1^{(J)} + \widetilde{[\epsilon^X, \epsilon^X]}_1^{(J)} + 2\widetilde{[X, \epsilon^X]}_1^{(J)} \right) \\ &= \frac{1}{K} \sum_{l=0}^{K-1} V_K^{(l)} - \frac{\bar{n}_K}{\bar{n}_J} \widetilde{[X, X]}_1^{(J)} + R_1 + R_2, \end{aligned} \quad (36)$$

where $R_1 = \widetilde{[\epsilon^X, \epsilon^X]}_1^{(K)} - \frac{\bar{n}_K}{\bar{n}_J} \widetilde{[\epsilon^X, \epsilon^X]}_1^{(1)}$, $R_2 = 2\widetilde{[X, \epsilon^X]}_1^{(K)} - 2\frac{\bar{n}_K}{\bar{n}_J} \widetilde{[X, \epsilon^X]}_1^{(1)}$, and

$$V_K^{(l)} = \sum_{j=1}^{\bar{n}_K} (X_{\tau_{jK+l}} - X_{\tau_{(j-1)K+l}})^2, \text{ for } l = 0, 1, \dots, K-1.$$

Note that we have assumed that $\bar{n}_K = \frac{n-K+1}{K}$ is an integer above, to simplify the presentation.

Recall that we consider the case when $J = 1$, or $\bar{n}_J = n$. We are interested in

$$\begin{aligned} &\sqrt{\bar{n}_K} (\widetilde{\langle X, X \rangle}_1 - \int_0^1 \sigma_t^2 dt) \\ &= \frac{1}{K} \sum_{l=0}^{K-1} \sqrt{\bar{n}_K} (V_K^{(l)} - \int_0^1 \sigma_t^2 dt) \\ &\quad - \left(\frac{\bar{n}_K}{n} \right)^{3/2} \cdot \sqrt{n} \left(\widetilde{[X, X]}_1^{(1)} - \int_0^1 \sigma_t^2 dt \right) \\ &\quad - \frac{\bar{n}_K^{3/2}}{n} \int_0^1 \sigma_t^2 dt + \sqrt{\bar{n}_K} R_1 + \sqrt{\bar{n}_K} R_2. \end{aligned} \quad (37)$$

The key idea is to compute the moment generating functions for each terms in (37) and then to use Lemma 2 to conclude.

For the first term in (37), since $V_k^{(l)}$ is a realized volatility based on discretely observed X process, with observation frequency satisfying $\sup_{1 \leq i \leq \bar{n}_K} \bar{n}_K \cdot (\tau_{iK+l} - \tau_{(i-1)K+l}) \leq C_\Delta$, we have, by (33) in Lemma 3, for $|\theta| \leq \frac{\sqrt{\bar{n}_K}}{4C_\sigma^2 C_\Delta}$,

$$E \exp\{\theta \sqrt{\bar{n}_K} (V_K^{(l)} - \int_0^1 \sigma_t^2 dt)\} \leq \exp\{2\theta^2 C_\sigma^4 C_\Delta^2\}. \quad (38)$$

For the second term in (37), we have obtained in (33) that

$$E \exp\{\theta \sqrt{n} (\widetilde{[X, X]}_1^{(1)} - \int_0^1 \sigma_t^2 dt)\} \leq \exp\{2\theta^2 C_\sigma^4 C_\Delta^2\}, \quad \text{when } |\theta| \leq \frac{\sqrt{n}}{4C_\sigma^2 C_\Delta}. \quad (39)$$

The third term in (37) can be ignored because it has an upper bound that goes to zero sufficiently fast as n grows:

$$\frac{\bar{n}_K^{3/2}}{n} \int_0^1 \sigma_t^2 dt \leq 2^{3/2} C_\sigma^2 / \sqrt{n}, \quad (40)$$

by Condition 5.

We introduce an auxiliary sequence a_n that grows with n in a moderate rate to facilitate our presentation in the following. In particular, we can set $a_n = n^{1/12}$.

Let us now deal with R_1 , the fourth term in (37). Note that from the definition

$$\begin{aligned}
& \sqrt{\bar{n}_K} R_1 \\
&= \frac{\sqrt{\bar{n}_K}}{K} \left\{ \sum_{i=K}^n (\epsilon_i - \epsilon_{i-K})^2 - \frac{n-K+1}{n} \sum_{i=1}^n (\epsilon_i - \epsilon_{i-1})^2 \right\} \\
&= \frac{\sqrt{\bar{n}_K} \sqrt{n}}{K} \cdot \frac{2}{\sqrt{n}} \sum_{i=1}^n \epsilon_i \epsilon_{i-1} \\
&\quad - \frac{\sqrt{\bar{n}_K} \sqrt{n-K+1}}{K} \cdot \frac{2}{\sqrt{n-K+1}} \sum_{i=K}^n \epsilon_i \epsilon_{i-K} \\
&\quad - \frac{\sqrt{\bar{n}_K} \sqrt{K-1} a_n}{K} \cdot \frac{1}{a_n \sqrt{K-1}} \sum_{i=1}^{K-1} (\epsilon_i^2 - \eta_X^2) \\
&\quad - \frac{\sqrt{\bar{n}_K} \sqrt{K-1} a_n}{K} \cdot \frac{1}{a_n \sqrt{K-1}} \sum_{i=n-K+1}^{n-1} (\epsilon_i^2 - \eta_X^2) \\
&\quad + \frac{\sqrt{\bar{n}_K} (K-1) a_n}{K \sqrt{n}} \cdot \frac{1}{a_n \sqrt{n}} \sum_{i=1}^n (\epsilon_i^2 - \eta_X^2) \\
&\quad + \frac{\sqrt{\bar{n}_K} (K-1) a_n}{K \sqrt{n}} \cdot \frac{1}{a_n \sqrt{n}} \sum_{i=0}^{n-1} (\epsilon_i^2 - \eta_X^2).
\end{aligned} \tag{41}$$

The first two terms in (41) are not the sum of independent variables. But they can be decomposed into the sum of independent random variables and the moment generating functions can be computed. To simplify the argument without losing the essential ingredient, let us focus on the first term of (41). It can be decomposed as

$$\sum_{i=1}^n \varepsilon_i \varepsilon_{i-1} = \sum_{\text{odd } i} \varepsilon_i \varepsilon_{i-1} + \sum_{\text{even } i} \varepsilon_i \varepsilon_{i-1}$$

and the summands in each terms of the right-hand side are now independent. Therefore, we need only to calculate the moment generating function of $\varepsilon_i \varepsilon_{i-1}$.

For two independent normally distributed random variables $X \sim N(0, \sigma_X^2)$ and $Y \sim N(0, \sigma_Y^2)$, it can easily be computed that

$$\begin{aligned}
E(\exp\{\theta n^{-1/2} XY\}) &= \left(\frac{1}{1 - \sigma_X^2 \sigma_Y^2 \theta^2 / n} \right)^{1/2} \\
&\leq \exp\{\sigma_X^2 \sigma_Y^2 \theta^2 / n\} \text{ when } |\theta| \leq \frac{\sqrt{n}}{\sqrt{2} \sigma_X \sigma_Y},
\end{aligned}$$

where we have used the fact that $\log(1-x) \geq -2x$ when $0 \leq x \leq \frac{1}{2}$.

Hence, by the independence, it follows that (we assume n is even to simplify the presentation)

$$\begin{aligned} E \exp \left\{ 2\theta n^{-1/2} \sum_{\text{odd } i} \varepsilon_i \varepsilon_{i-1} \right\} &= \left(\frac{1}{1 - 4\eta_X^4 \theta^2 / n} \right)^{n/4} \\ &\leq \exp \{ 2\eta_X^4 \theta^2 \}, \text{ when } |\theta| \leq \frac{\sqrt{n}}{2\sqrt{2}\eta_X^2}. \end{aligned} \quad (42)$$

The second term in R_1 works similarly and have the same bound. For example, when \bar{n}_K is even, one can have the following decomposition

$$\sum_{i=K}^n \epsilon_i \epsilon_{i-K} = \sum_{j=1}^{\bar{n}_K/2} \sum_{i=2jK-K}^{2jK-1} \epsilon_i \epsilon_{i-K} + \sum_{j=1}^{\bar{n}_K/2} \sum_{i=2jK}^{2jK+K-1} \epsilon_i \epsilon_{i-K}.$$

The last four terms are sums of independent χ^2 -distributed random variables and their moment generating functions can easily be bounded by using Lemma 1. Taking the term $\frac{1}{a_n \sqrt{K-1}} \sum_{i=1}^{K-1} (\epsilon_i^2 - \eta_X^2)$ for example, we have

$$E \left(\exp \left\{ \frac{\theta}{a_n \sqrt{K-1}} \sum_{i=1}^{K-1} (\epsilon_i^2 - \eta_X^2) \right\} \right) \leq \exp \{ 2\eta_X^4 \theta^2 / a_n^2 \} \text{ when } |\theta| \leq \frac{a_n \sqrt{K-1}}{4\eta_X^2}.$$

For the term R_2 , we have,

$$\begin{aligned} \sqrt{\bar{n}_K} R_2 &= \frac{2a_n \bar{n}_K}{n} \frac{1}{a_n} \left(\sum_{i=1}^n \Delta X_i \epsilon_{i-1} - \sum_{i=1}^n \Delta X_i \epsilon_i \right) \\ &\quad + \frac{2}{a_n} \cdot \frac{a_n \sqrt{\bar{n}_K}}{K} \left(\sum_{i=K}^n \Delta^{(K)} X_i \epsilon_i - \sum_{i=K}^n \Delta^{(K)} X_i \epsilon_{i-K} \right), \end{aligned} \quad (43)$$

where $\Delta X_i = X_{\tau_i} - X_{\tau_{i-1}}$, and $\Delta^{(K)} X_i = X_{\tau_i} - X_{\tau_{i-K}}$. The first term above satisfies

$$\begin{aligned} E \left(\exp \left\{ \frac{\theta}{a_n} \sum_{i=1}^n \Delta X_i \epsilon_i \right\} \right) &= E \left(\exp \left\{ \sum_{i=1}^n \left(\frac{\theta}{a_n} \Delta X_i \right)^2 \eta_X^2 / 2 \right\} \right) \\ &\leq \left(E \left(\exp \{ \theta^2 \eta_X^2 C_\sigma^2 C_\Delta Z^2 / 2na_n^2 \} \right) \right)^n \\ &= \left(\frac{1}{1 - \eta_X^2 C_\sigma^2 C_\Delta \theta^2 / na_n^2} \right)^{n/2} \\ &\leq \exp \{ \eta_X^2 C_\sigma^2 C_\Delta \theta^2 / a_n^2 \}, \text{ when } |\theta| \leq \frac{\sqrt{n} a_n}{\sqrt{2} C_\Delta C_\sigma \eta_X}, \end{aligned} \quad (44)$$

where in the second line we have again used the optional sampling theorem and law of iterated expectations as in the derivations of Lemma 3; Z denotes a standard normal random variable. The

second term in R_2 works similarly and has the same bound. For the third term, we have

$$\begin{aligned}
& E \left[\exp \left\{ \frac{a_n \theta \sqrt{\bar{n}_K}}{K} \sum_{i=K}^n \Delta^{(K)} X_i \epsilon_i \right\} \right] \\
&= E \left[E \left(\exp \left\{ \frac{a_n \theta \sqrt{\bar{n}_K}}{K} \sum_{i=K}^n \Delta^{(K)} X_i \epsilon_i \right\} \middle| \mathbf{X} \text{ process} \right) \right] \\
&= E \left[\exp \left\{ \frac{a_n^2 \theta^2 \bar{n}_K}{2K^2} \sum_{l=0}^{K-1} \sum_{j=1}^{\bar{n}_K} (\Delta^{(K)} X_i)^2 \eta_X^2 \right\} \right] \\
&\leq \prod_{l=0}^{K-1} \left\{ E \left[\exp \left\{ \frac{a_n^2 \theta^2 \bar{n}_K \eta_X^2}{2K} \sum_{j=1}^{\bar{n}_K} (\Delta^{(K)} X_i)^2 \right\} \right] \right\}^{\frac{1}{K}} \\
&\leq \prod_{l=0}^{K-1} \left\{ \left(1 - \frac{a_n^2 \theta^2 \eta_X^2}{K} C_\sigma^2 C_\Delta \right)^{-\bar{n}_K/2} \right\}^{\frac{1}{K}} \\
&\leq \exp \left\{ \frac{a_n^2 \theta^2 \bar{n}_K \eta_X^2}{K} C_\sigma^2 C_\Delta \right\} \text{ when } |\theta| \leq \frac{\sqrt{K}}{\sqrt{2C_\Delta} a_n \eta C_\sigma},
\end{aligned} \tag{45}$$

where we have used the Hölder's inequality above. The forth term works similarly and has the same bound.

Combining the results for all the terms (38) – (45) together, applying Lemma 2 to (37), we have, for the following set of parameters, the conditions for Lemma 2 are satisfied with $C_1 = C_{1,x} \sqrt{\bar{n}_K}$.

$$\begin{aligned}
C_{1,x} &= \min \left\{ \frac{1}{4C_\sigma^2 C_\Delta}, \frac{\sqrt{n/\bar{n}_K}}{2\sqrt{2}\eta_X^2}, \frac{a_n \sqrt{(K-1)/\bar{n}_K}}{4\eta_X^2}, \frac{a_n \sqrt{n/\bar{n}_K}}{\sqrt{2C_\Delta} \eta_X C_\sigma}, \frac{\sqrt{K/\sqrt{\bar{n}_K}}}{\sqrt{2C_\Delta} a_n \eta C_\sigma} \right\} \\
&= \frac{1}{4C_\sigma^2 C_\Delta} \text{ for big enough } n,
\end{aligned} \tag{46}$$

$$\begin{aligned}
C_2 &= \max \{ 2C_\sigma^4 C_\Delta^2, 2\eta_X^4, 2\eta_X^4/a_n^2, \eta_X^2 C_\sigma^2 C_\Delta/a_n^2, \frac{a_n^2 \bar{n}_K \eta_X^2}{K} C_\sigma^2 C_\Delta \} \\
&= \max \{ 2C_\sigma^4 C_\Delta^2, 2\eta_X^4 \} \text{ for big enough } n \\
&= 2C_\sigma^4 C_\Delta^2 \text{ considering the values } C_\Delta \geq 1, C_\sigma \geq \eta_X \text{ typically,}
\end{aligned} \tag{47}$$

and

$$\begin{aligned}
w &= 14 = \lceil 2 + 8\sqrt{2} \rceil \\
&> \underbrace{\frac{1}{K} \sum_{l=0}^{K-1} 1 + \left(\frac{\bar{n}_K}{n} \right)^{3/2}}_{\text{coefficients in the first two terms of (37)}} \\
&\quad + \underbrace{\frac{4\sqrt{\bar{n}_K} \sqrt{n}}{K} + \frac{2\sqrt{\bar{n}_K} a_n}{\sqrt{K}} + \frac{2\sqrt{\bar{n}_K} a_n}{\sqrt{n}}}_{\text{controls coefficients in (41)}} + \underbrace{\frac{4a_n \bar{n}_K}{n} + \frac{4}{a_n}}_{\text{coefficients in (43)}},
\end{aligned}$$

where the $>$ is valid when n is big enough and Condition 5 is applied.

By Lemma 2, when $0 \leq x \leq 2C_{1,x}C_2\sqrt{\bar{n}_K}$,

$$P\{\sqrt{\bar{n}_K}|\widehat{\langle X, X \rangle}_1 - \int_0^1 \sigma_t^2 dt| > x\} \leq 4 \exp(-(16C_2w^2)^{-1}x^2).$$

By the Condition 5 again, we have

$$\begin{aligned} P\{n^{1/6}|\widehat{\langle X, X \rangle}_1 - \int_0^1 \sigma_t^2 dt| > x\} &\leq P(\sqrt{\bar{n}_K}|\widehat{\langle X, X \rangle}_1 - \int_0^1 \sigma_t^2 dt| > x/\sqrt{2}) \\ &\leq 4 \exp(-Cx^2), \quad \text{when } 0 \leq x \leq cn^{1/6}, \end{aligned} \quad (48)$$

where

$$c = 2C_{1,x}C_2 \text{ and } C = (32C_2w^2)^{-1}. \quad (49)$$

This completes the proof of the result conditional on the observation times. Theorem 1 is proved by noting that this conditional result depend only on the observation frequency n and not on the locations of the observation times as long as the Condition 3 is satisfied.

Note also that in the above proof, we have demonstrated by using a sequence a_n that goes to ∞ at a moderate rate that, one can eliminate the impact of the small order terms on the choices of the constants, as long as the terms have their moment generating functions satisfy inequalities of form (27). We will use this technique again in the next subsection.

A.4 Proof of Theorem 2

We again conduct all the analysis assuming the observation times are given. Our final result holds because the conditional result doesn't depend on the locations of the observation times as long as the Condition 3 is satisfied.

Recall notation for the observation times as introduced in section 3.2. Define

$$Z^+ = X + Y \quad \text{and} \quad Z^- = X - Y.$$

Z^+ and Z^- are diffusion processes with bounded volatility. To see this, let W^+ and W^- be processes such that

$$dW_t^+ = \frac{\sigma_t^{(X)}dB_t^{(X)} + \sigma_t^{(Y)}dB_t^{(Y)}}{\sqrt{(\sigma_t^{(X)})^2 + (\sigma_t^{(Y)})^2 + 2\rho_t\sigma_t^{(X)}\sigma_t^{(Y)}}}$$

and

$$dW_t^- = \frac{\sigma_t^{(X)}dB_t^{(X)} - \sigma_t^{(Y)}dB_t^{(Y)}}{\sqrt{(\sigma_t^{(X)})^2 + (\sigma_t^{(Y)})^2 - 2\rho_t\sigma_t^{(X)}\sigma_t^{(Y)}}}.$$

W^+ and W^- are standard Brownian motions by Levy's characterization of Brownian motion (see,

for example, Theorem 3.16 of Karatzas and Shreve (2000)). Write

$$\sigma_t^{Z^+} = \sqrt{(\sigma_t^{(X)})^2 + (\sigma_t^{(Y)})^2 + 2\rho_t \sigma_t^{(X)} \sigma_t^{(Y)}}$$

and

$$\sigma_t^{Z^-} = \sqrt{(\sigma_t^{(X)})^2 + (\sigma_t^{(Y)})^2 - 2\rho_t \sigma_t^{(X)} \sigma_t^{(Y)}},$$

we have

$$dZ^+ = \sigma_t^{Z^+} dW_t^+ \text{ and } dZ^- = \sigma_t^{Z^-} dW_t^-$$

with $0 \leq \sigma_t^{Z^+}, \sigma_t^{Z^-} \leq 2C_\sigma$.

For the observed Z^+ and Z^- processes, we have

$$Z_{v_i}^{+,o} = X_{t_i}^o + Y_{s_i}^o = Z_{v_i}^+ + \epsilon_{i,+} \text{ and } Z_{v_i}^{-,o} = X_{t_i}^o - Y_{s_i}^o = Z_{v_i}^- + \epsilon_{i,-},$$

where t_i and s_i are the last ticks at or before v_i and

$$\begin{aligned} \epsilon_{i,+} &= X_{t_i} - X_{v_i} + Y_{s_i} - Y_{v_i} + \epsilon_i^X + \epsilon_i^Y, \\ \epsilon_{i,-} &= X_{t_i} - X_{v_i} - Y_{s_i} + Y_{v_i} + \epsilon_i^X - \epsilon_i^Y. \end{aligned}$$

Note that

$$\widehat{\langle X, Y \rangle}_1 = \frac{1}{4}(\widehat{\langle Z^+, Z^+ \rangle}_1 - \widehat{\langle Z^-, Z^- \rangle}_1).$$

We can first prove analogues results as Theorem 1 for $\widehat{\langle Z^+, Z^+ \rangle}_1$ and $\widehat{\langle Z^-, Z^- \rangle}_1$, then utilize the results to obtain the final conclusion for TSCV.

For $\widehat{\langle Z^+, Z^+ \rangle}_1$, the derivation is different from that of Theorem 1 only for the terms that involve the noise, namely $\sqrt{\tilde{n}_K}R_1$ and $\sqrt{\tilde{n}_K}R_2$. Write $\tilde{\Delta}X_i = X_{t_i} - X_{v_i}$ and $\tilde{\Delta}Y_i = Y_{s_i} - Y_{v_i}$. Then, we have, the first term in $\sqrt{\tilde{n}_K}R_1$ becomes

$$\begin{aligned} & \frac{\sqrt{\tilde{n}_K}\sqrt{\tilde{n}}}{K} \cdot \frac{2}{\sqrt{\tilde{n}}} \sum_{i=1}^{\tilde{n}} \epsilon_{i,+} \epsilon_{i-1,+} \\ &= \frac{\sqrt{\tilde{n}_K}\sqrt{\tilde{n}}}{K} \cdot \frac{2}{\sqrt{\tilde{n}}} \sum_{i=1}^{\tilde{n}} \left(\tilde{\Delta}X_i \tilde{\Delta}X_{i-1} + \tilde{\Delta}X_i \tilde{\Delta}Y_{i-1} + \tilde{\Delta}X_i (\epsilon_{i-1}^X + \epsilon_{i-1}^Y) \right. \\ & \quad + \tilde{\Delta}Y_i \tilde{\Delta}X_{i-1} + \tilde{\Delta}Y_i \tilde{\Delta}Y_{i-1} + \tilde{\Delta}Y_i (\epsilon_{i-1}^X + \epsilon_{i-1}^Y) + (\epsilon_i^X + \epsilon_i^Y) \tilde{\Delta}X_{i-1} \\ & \quad \left. + (\epsilon_i^X + \epsilon_i^Y) \tilde{\Delta}Y_{i-1} + (\epsilon_i^X + \epsilon_i^Y) (\epsilon_{i-1}^X + \epsilon_{i-1}^Y) \right) \end{aligned}$$

The only $O_P(1)$ term is the last term, which involves only independent normals, and can be dealt

with by the same way as before (again assume \tilde{n} is even for the simplicity of presentation below):

$$\begin{aligned}
& E \exp \left\{ 2\theta n^{-1/2} \sum_{\text{odd } i} (\epsilon_i^X + \epsilon_i^Y)(\epsilon_{i-1}^X + \epsilon_{i-1}^Y) \right\} \\
&= E \exp \left\{ 2\theta \tilde{n}^{-1/2} \sum_{\text{even } i} (\epsilon_i^X + \epsilon_i^Y)(\epsilon_{i-1}^X + \epsilon_{i-1}^Y) \right\} \\
&= \left(\frac{1}{1 - 4(\eta_X^2 + \eta_Y^2)^2 \theta^2 / \tilde{n}} \right)^{\tilde{n}/4} \\
&\leq \exp \{ 2(\eta_X^2 + \eta_Y^2)^2 \theta^2 \}, \text{ when } |\theta| \leq \frac{\sqrt{\tilde{n}}}{2\sqrt{2}(\eta_X^2 + \eta_Y^2)}.
\end{aligned}$$

The other terms are of a smaller order of magnitude. By applying an $a_{\tilde{n}}$ sequence which grows moderately with \tilde{n} as in the proof of Theorem 1 (we can set $a_{\tilde{n}} = \tilde{n}^{1/12}$), we can see easily that their exact bounds don't have effect on our choice of C_1 , C_2 or ω . All we need to show is that the moment generating functions of these terms can indeed be suitably bounded as (27). To show this, first note that, for any positive number a and real valued b , by the optional sampling theorem (applied to sub-martingales $\exp(aB_s^2)$ and $\exp(b\tilde{\Delta}yB_s)$ with stopping time $[X]_u \leq C_\sigma^2 u$ for real number $\tilde{\Delta}y$), we have,

$$\begin{aligned}
E \left(\exp \{ a(\tilde{\Delta}X_i)^2 \} | \mathcal{F}_{i-1} \right) &\leq \left(E \left(\exp \{ aC_\sigma^2 C_\Delta Z^2 / \tilde{n} \} \right) \right) \text{ for } Z \sim N(0, 1) \\
&= \left(\frac{1}{1 - 2aC_\sigma^2 C_\Delta / \tilde{n}} \right)^{1/2},
\end{aligned} \tag{50}$$

where \mathcal{F}_i is the information collected up to time v_i . Inequality (50) holds when $\tilde{\Delta}X_i$ is replaced by $\tilde{\Delta}Y_i$. Similarly,

$$\begin{aligned}
E \left(\exp \{ b\tilde{\Delta}X_i \tilde{\Delta}Y_{i-1} \} | \mathcal{F}_{i-2} \right) &\leq E \left(E \left(\exp \{ b\tilde{\Delta}X_i \tilde{\Delta}Y_{i-1} \} | \mathcal{F}_{i-1} \right) | \mathcal{F}_{i-2} \right) \\
&\leq E \left(\exp \{ b^2 C_\Delta C_\sigma^2 (\tilde{\Delta}Y_{i-1})^2 / 2\tilde{n} \} | \mathcal{F}_{i-2} \right) \\
&\leq \left(\frac{1}{1 - b^2 C_\Delta^4 C_\sigma^2 / \tilde{n}^2} \right)^{1/2}.
\end{aligned} \tag{51}$$

The inequalities (50) and (51) can be used to obtain the bounds we need. For example, by (51) and the law of iterated expectations,

$$\begin{aligned}
E \left(\exp \{ \theta \sum_{\text{odd } i} \tilde{\Delta}X_i \tilde{\Delta}Y_{i-1} \} \right) &\leq \left(\frac{1}{1 - \theta^2 C_\sigma^4 C_\Delta^2 / \tilde{n}^2} \right)^{\tilde{n}/4} \\
&\leq \exp \{ \theta^2 C_\sigma^4 C_\Delta^2 / 2\tilde{n} \} \text{ when } |\theta| \leq \frac{\tilde{n}}{\sqrt{2} C_\sigma^2 C_\Delta};
\end{aligned}$$

by independence, normality of the noise, the law of iterated expectations and (50), we have

$$\begin{aligned}
& E\left(\exp\left\{\frac{\theta}{a_{\tilde{n}}} \sum_{i=1}^{\tilde{n}} \tilde{\Delta} X_i (\epsilon_{i-1}^X + \epsilon_{i-1}^Y)\right\}\right) \\
&= E\left(\exp\left\{\sum_{i=1}^{\tilde{n}} \left(\frac{\theta}{a_{\tilde{n}}} \tilde{\Delta} X_i\right)^2 (\eta_X^2 + \eta_Y^2)/2\right\}\right) \\
&\leq \left(\frac{1}{1 - (\eta_X^2 + \eta_Y^2)\theta^2 C_\sigma^2 C_\Delta / \tilde{n} a_{\tilde{n}}^2}\right)^{\tilde{n}/2} \\
&\leq \exp\{(\eta_X^2 + \eta_Y^2) C_\sigma^2 C_\Delta \theta^2 / a_{\tilde{n}}^2\}, \text{ when } |\theta| \leq \frac{\sqrt{\tilde{n} a_{\tilde{n}}}}{C_\sigma \sqrt{2 C_\Delta (\eta_X^2 + \eta_Y^2)}}.
\end{aligned}$$

Similar results can be found for the other terms above, with the same techniques.

The second term in $\sqrt{n_K} R_1$ works similarly and have the same bound. The other terms in $\sqrt{n_K} R_1$ and the whole term of $\sqrt{n_K} R_2$ are of order $o_P(1)$. Again, by using a sequence $a_{\tilde{n}}$ we can conclude immediately that their exact bounds won't matter in our choice of the constants and we only need to show that their moment generating functions are appropriately bounded as (27). The arguments needed to prove the inequalities of form (27) for each elements in these terms are similar to those presented in the above proofs, and are omitted here.

Hence, by still letting $w = 14$ and redefining

$$\begin{aligned}
C_{1,x} &= \frac{1}{4(2C_\sigma)^2 C_\Delta} \quad \text{and} \\
C_2 &= \max\{2(2C_\sigma)^4 C_\Delta^2, 2(\eta_X^2 + \eta_Y^2)^2\} \\
&= 32C_\sigma^4 C_\Delta^2 \text{ for the typical case when } C_\sigma \geq \eta_X, \eta_Y,
\end{aligned}$$

we have, when $0 \leq x \leq c' \tilde{n}^{1/6}$,

$$\begin{aligned}
& P\{\tilde{n}^{1/6} |\widehat{\langle Z^+, Z^+ \rangle}_1 - \int_0^1 \sigma_t^{Z^+2} dt| > x\} \leq 4 \exp(-C' x^2), \\
& \text{and } P\{\tilde{n}^{1/6} |\widehat{\langle Z^-, Z^- \rangle}_1 - \int_0^1 \sigma_t^{Z^-2} dt| > x\} \leq 4 \exp(-C' x^2),
\end{aligned}$$

where

$$c' = 2C_{1,x} C_2 \text{ and } C' = (32C_2 w^2)^{-1}.$$

Finally, for the TSCV estimator, when $0 \leq x \leq c\tilde{n}^{1/6}$,

$$\begin{aligned}
& P\{\tilde{n}^{1/6}|\widehat{\langle X, Y \rangle}_1 - \int_0^1 \sigma_t^{(X)} \sigma_t^{(Y)} \rho_t^{(X,Y)} dt| > x\} \\
& \leq P\{\tilde{n}^{1/6}|\widehat{\langle Z^+, Z^+ \rangle}_1 - \int_0^1 \sigma_t^{Z^+2} dt| > 2x\} \\
& \quad + P\{\tilde{n}^{1/6}|\widehat{\langle Z^-, Z^- \rangle}_1 - \int_0^1 \sigma_t^{Z^-2} dt| > 2x\} \\
& \leq 8 \exp(-Cx^2),
\end{aligned}$$

where

$$c = c'/2 = C_{1,x}C_2 \text{ and } C = 4C' = (8C_2w^2)^{-1}. \quad (52)$$

This completes the proof.

Note that the argument is not restricted to TSCV based on the pairwise refresh times – it works the same (only with \tilde{n} replaced by \tilde{n}_* , the observation frequency of the all-refresh method) for the case when the synchronization scheme is chosen to be the all-refresh method, as long as the sampling conditions Condition 3-4 are satisfied.

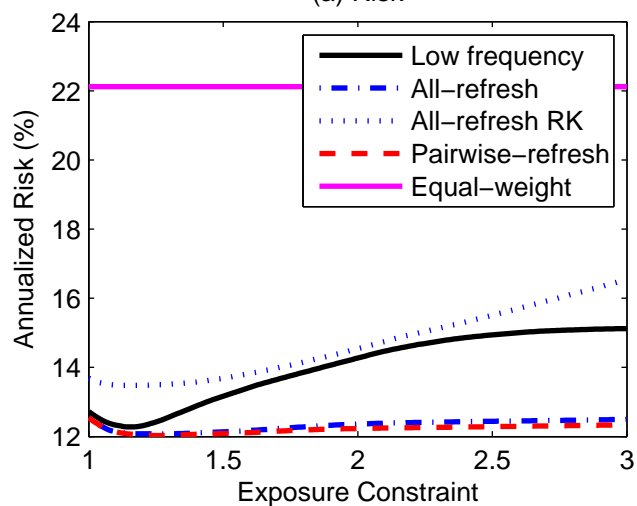
REFERENCES

- Aït-Sahalia, Y., Mykland, P. A. and Zhang, L. (2005). How often to sample a continuous-time process in the presence of market microstructure noise. *Review of Financial Studies*, **18**, 351-416.
- Aït-Sahalia, Y., Fan, J., Xiu, D. (2010). High Frequency Covariance Estimates with Noisy and Asynchronous Financial Data
- Andersen, T.G., Bollerslev, T., Diebold, F.X. and Labys, P. (2000). Great realizations. *Risk*, **13**, 105-108.
- Barndorff-Nielsen, O. E., Hansen, P. R., Lunde, A., and Shephard, N. (2008). Multivariate realised kernels: consistent positive semi-definite estimators of the covariation of equity prices with noise and non-synchronous trading. *Manuscript*.
- Barndorff-Nielsen, O. E., Hansen, P. R., Lunde, A., and Shephard, N. (2009). Realized kernels in practice: trades and quotes. *Economet. Jour.*, **12**, 1-32.
- Barndorff-Nielsen, O. E., Hansen, P. R., Lunde, A., and Shephard, N. (2009b). Subsampling realised kernel. *Jour. Econ.*, to appear.
- Best, M.J. and Grauer, R.R. (1991). On the sensitivity of mean-variance-efficient portfolios to changes in asset means: Some analytical and computational results. *Review of Financial Studies*, **2**, 315-342.

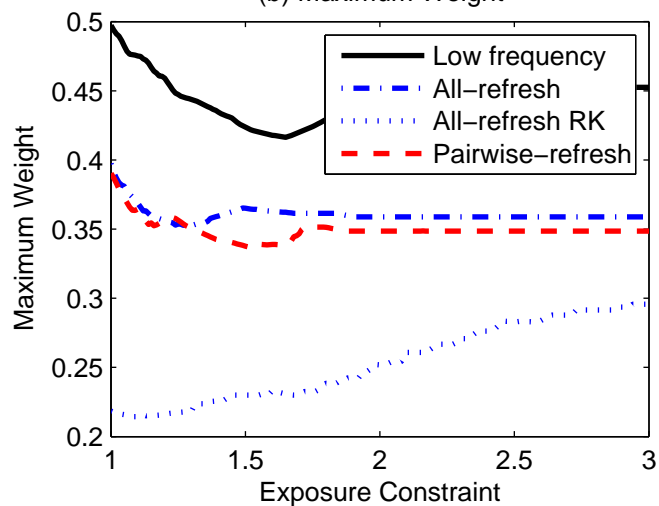
- Bickel, P. J. and Levina, E. (2008). Regularized estimation of large covariance matrices. *Ann. Statist.*, **36**, 199-227.
- Chopra, V.K. and Ziemba, W.T. (1993). The effect of errors in means, variance and covariances on optimal portfolio choice. *Journal of Portfolio Management*, winter, 6-11.
- Delbaen, F. and Schachermayer, W. (1994). A general version of the fundamental theorem of asset pricing. *Mathematische Annalen*, **300**, 463-520.
- De Roon, F. A., Nijman, T.E., and Werker, B.J.M. (2001). Testing for mean-variance spanning with short sales constraints and transaction costs: The case of emerging markets. *Journal of Finance*, **54**, 721-741.
- Epps, T.W. (1979). Comovements in stock prices in the very short run. *Jour. Ameri. Statist. Assoc.*, **74**, 291-298.
- Fan, J. and Wang, Y. (2007). Multi-scale jump and volatility analysis for high-Frequency financial data.
- Fan, J., Fan, Y. and Lv, J. (2008). Large dimensional covariance matrix estimation via a factor model. *Journal of Econometrics*, **147**, 186-197.
- Fan, J., Zhang, J., and Yu, K. (2008). Asset Allocation and Risk Assessment with Gross Exposure Constraints for Vast Portfolios. *Manuscript*.
- Hayashi, T. and Yoshida, N. (2005). On covariance estimation of non-synchronously observed diffusion processes. *Bernoulli*, **11**, 359-379.
- Jagannathan, R. and Ma, T. (2003). Risk reduction in large portfolios: Why imposing the wrong constraints helps. *Journal of Finance*, **58**, 1651-1683.
- Jacod, J., Li, Y., Mykland, P.A., Podolskij, M., Vetter, M. (2009). Microstructure Noise in the continuous case: The Pre-averaging approach. *Stochastic Processes and their Applications*, **119**, 2249-2276.
- Jacod, J. and Shiryaev, A. N. (2003). *Limit Theorems for Stochastic Processes* (2nd edition). Springer-Verlag, New York.
- Johnstone, I. M. (2001). On the distribution of the largest eigenvalue in principal components analysis. *Ann. Statist.*, **29**, 295-327.
- Karatzas, I. and Shreve, S. E. (2000). *Brownian Motion and Stochastic Calculus* (2nd ed.). Springer, New York.
- Kinnebrock, S, Podolskij, M., and Christensen, K. (2009). Pre-Averaging estimators of the ex-post covariance matrix in noisy diffusion models with non-synchronous data. *Manuscript*

- Klein, R.W. and Bawa, V.S. (1976). The effect of estimation risk on optimal portfolio choice. *Journal of Financial Economics*, **3**, 215-231.
- Lam, C. and Fan, J. (2009). Sparsistency and rates of convergence in large covariance matrices estimation. *The Annals of Statistics*, **37**, 4254-4278.
- Li, Y. and Mykland, P. (2007). Are volatility estimators robust with respect to modeling assumptions? *Bernoulli*, **13**, 601-622.
- Markowitz, H. M. (1952). Portfolio selection. *Journal of Finance* **7** 77-91.
- Markowitz, H. (1959). *Portfolio Selection: Efficient Diversification of Investments*. John Wiley & Sons, New York.
- Rothman, A.J., Levina, E. and Zhu, J. (2009). Generalized thresholding of large covariance matrices. *Jour. Amer. Statist. Assoc.*, to appear.
- Wang, Y. Yao, Y., Zou, J. and Li, P. (2008). High dimensional volatility modeling and analysis for high-frequency financial data. *Manuscript*
- Xiu, D. (2008). Quasi-maximum likelihood estimation of volatility with high frequency data. *Manuscript*.
- Zhang, L. (2006). Efficient estimation of stochastic volatility using noisy observations: a multi-scale approach. *Bernoulli*, **12**, 1019-1043.
- Zhang, L. (2009). Estimating covariation: Epps effect and microstructure noise. *Journal of Econometrics*, to appear.
- Zhang, L., Mykland, P. A. and Aït-Sahalia, Y. (2005). A Tale of Two Time Scales: Determining Integrated Volatility with Noisy High-Frequency Data,” *Journal of the American Statistical Association*, 100, 1394-1411.

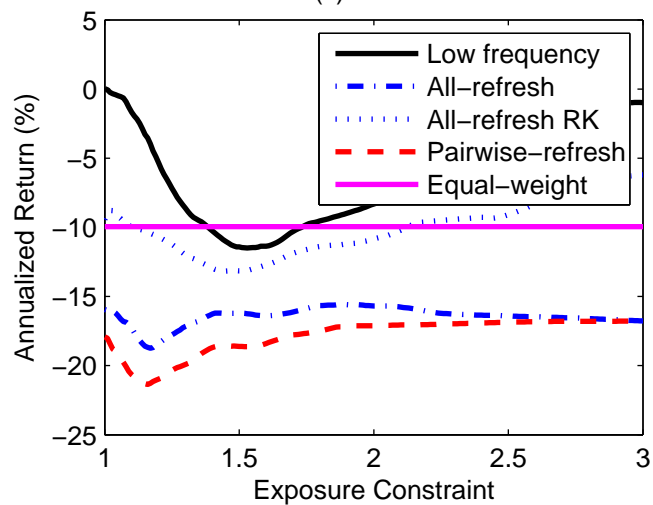
(a) Risk



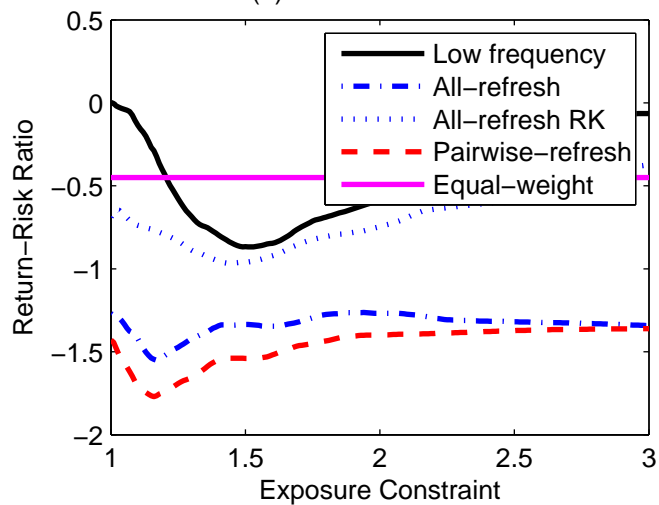
(b) Maximum Weight



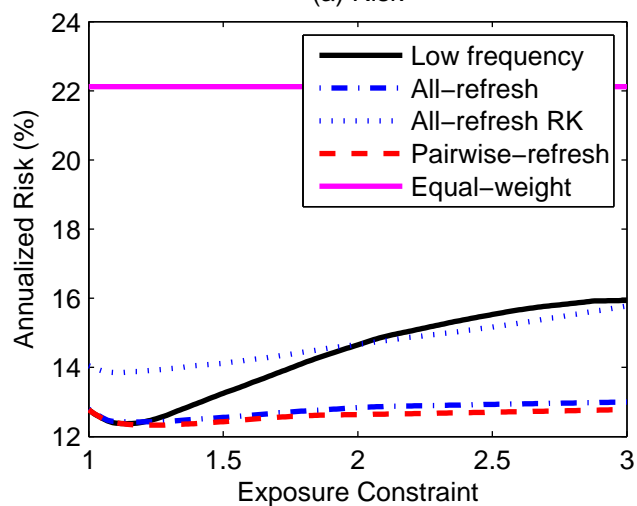
(c) Return



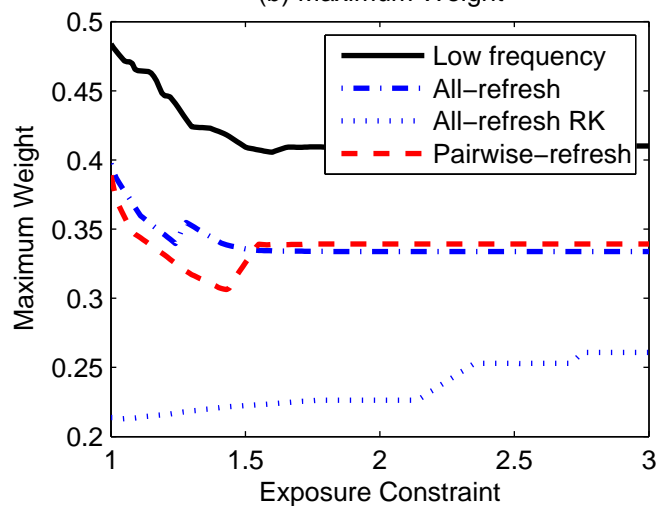
(d) Return-Risk Ratio



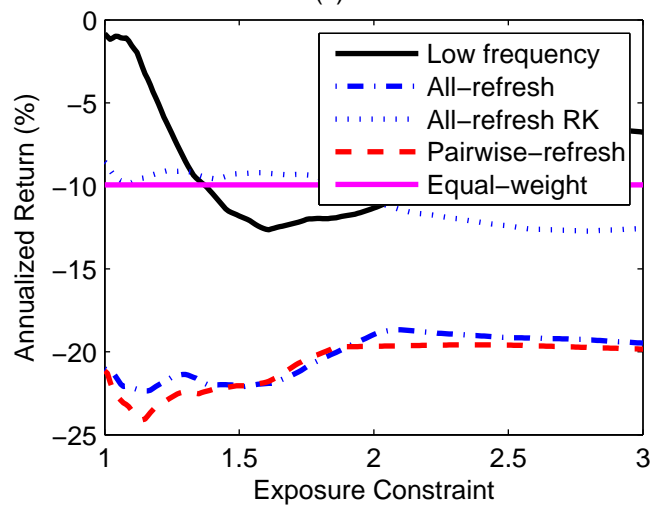
(a) Risk



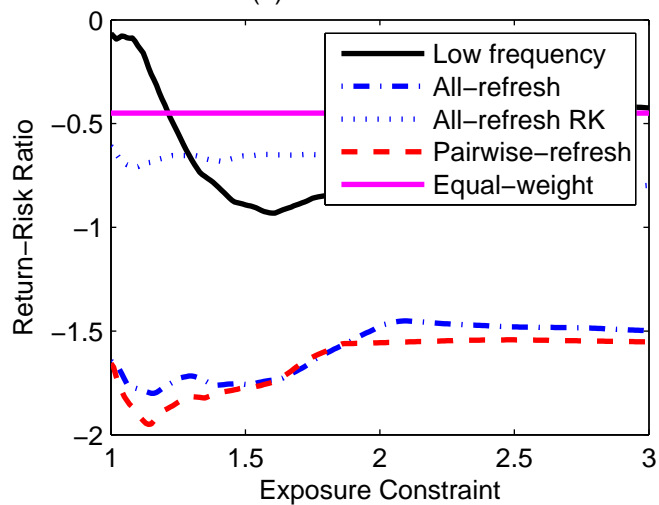
(b) Maximum Weight



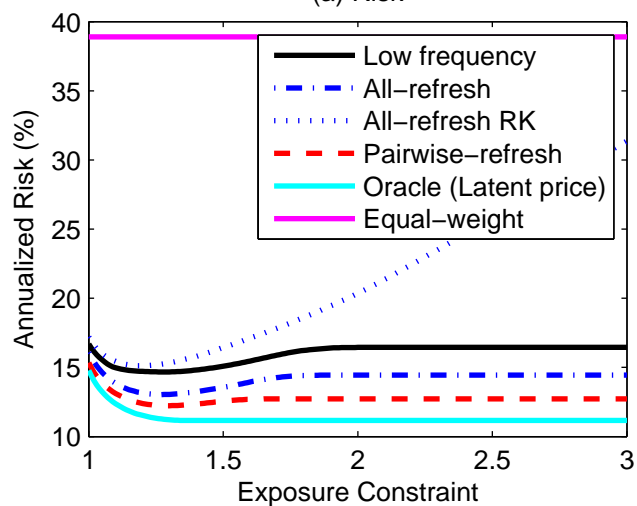
(c) Return



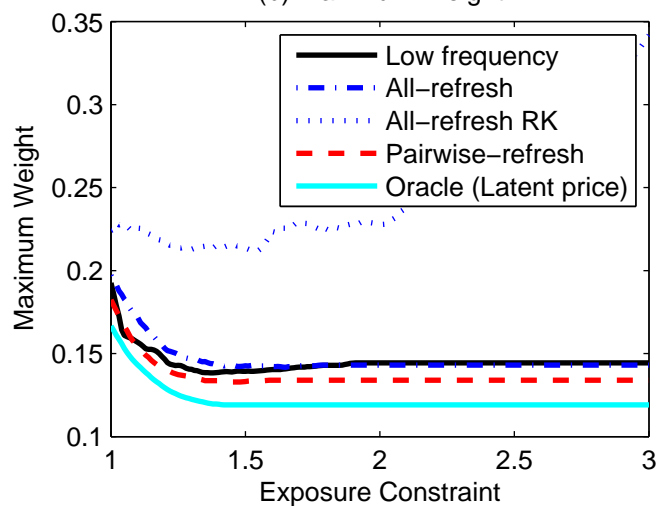
(d) Return-Risk Ratio



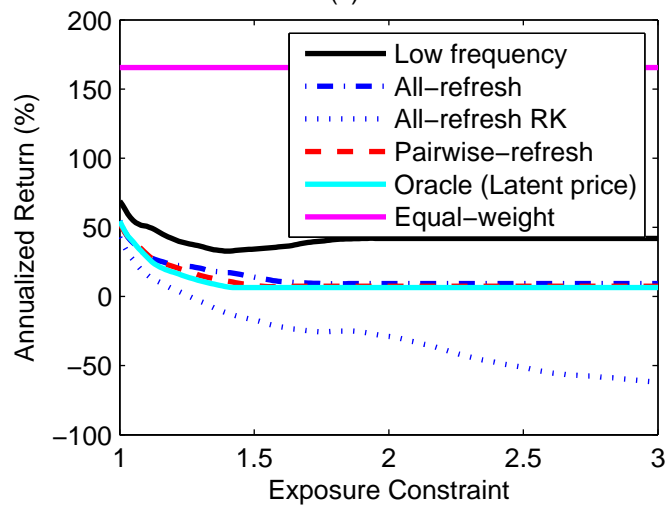
(a) Risk



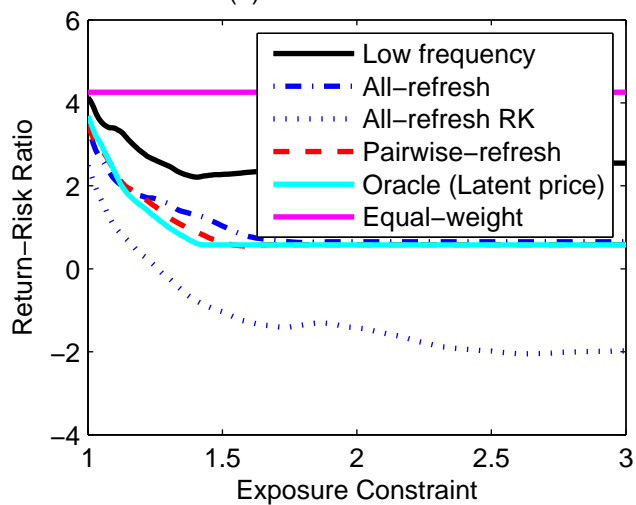
(b) Maximum Weight



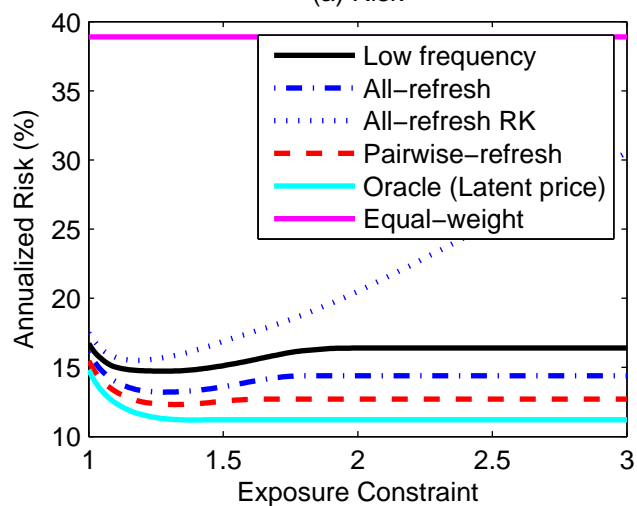
(c) Return



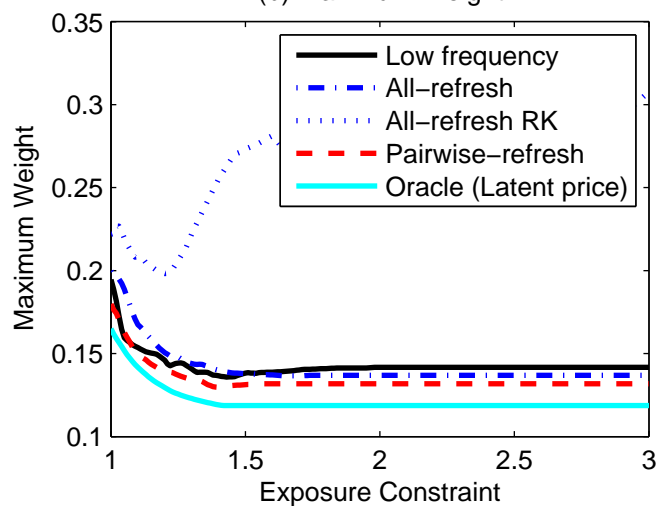
(d) Return-Risk Ratio



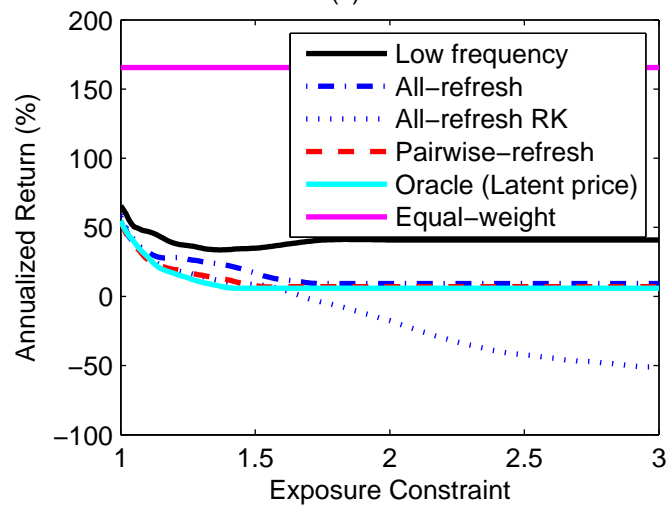
(a) Risk



(b) Maximum Weight



(c) Return



(d) Return-Risk Ratio

